Babeş-Bolyai University

Cluj-Napoca

Faculty of Chemistry and Chemical Engineering

Doctoral School of Chemistry

Protein engineering of phenylalanine ammonia-lyases for the synthesis of arylalanines of high synthetic importance

PhD Thesis Abstract

PhD candidate: Emma Zsófia Aletta Nagy

Scientific advisor: Prof. Habil. Dr. Eng. Csaba Paizs

Cluj Napoca

2021

Babeş-Bolyai University

Cluj-Napoca

Faculty of Chemistry and Chemical Engineering

Doctoral School of Chemistry

Protein engineering of phenylalanine ammonia-lyases for the synthesis of arylalanines of high synthetic importance

PhD Thesis Abstract

PhD candidate: Emma Zsófia Aletta Nagy

President: Prof. Dr. Cristian Sorin Silvestru – *member of the Romanian Academy, Babeş-Bolyai University, Cluj-Napoca*

Scientific advisor: Prof. Habil. Dr. Eng. Csaba Paizs – *Babeş-Bolyai University, Cluj-Napoca*

Reviewers: Prof. Dr. Ionel Mangalagiu – *„Alexandru Ioan Cuza" University of Iaşi*

Assoc. Prof. Dr. Mădălina Valentina Săndulescu-Tudorache – *University of Bucharest*

Prof. Dr. Ion Grosu – *corresponding member of Romanian Academy – Babeş-Bolyai University, Cluj-Napoca*

Cluj Napoca

2021

Table of Contents

1. Introduction 4
1.1. Optically pure amino acids 4
1.2. Phenylalanine ammonia lyase from *Petroselinum crispum* (*Pc*PAL) 5
1.3. Coupling the PAL-catalyzed reactions with the FDC1-catalyzed decarboxylation 6
1.3.1. Ferulic acid decarboxylase (FDC1) from Saccharomyces cerevisiae 7
2. Aims of the study 9
3. Results and discussion 12
3.1. Chemical synthesis of substrates and development of the analytical methods used for monitoring the enzymatic reactions 12
3.1.1. Chemical synthesis of racemic amino acids *rac*-2a-l 12
3.1.2. Chemical synthesis of acrylic acids 12
3.1.3. Synthesis of the fluorogenic diaryltetrazole probe 13
3.1.4. HPLC methods for the conversion determination of PAL-mediated biotransformations 14
3.1.5. HPLC methods for the conversion determination of FDC1-mediated biotransformations 14
3.2. Rational design-based protein engineering of PAL from *Petroselinum crispum* 15
3.2.1. Generating a library of *Pc*PAL single mutants through rational design 15
3.2.2. Screening the activity and selectivity of the *Pc*PAL-mutant library 15
3.2.3. Enzyme kinetic measurements 19
3.2.4. Synthetic aplicability of the engineered *Pc*PAL variants. 20
3.2.5. Crystallization studies 21
3.2.6. Conclusions 22
3.3. Development of high-throughput PAL-activity assay applicable for directed evolution based protein engineering 22
3.3.1. Exploring and extending the substrate scope of ferulic acid decarboxylase for ensuring compatibility with the substrate domain of PALs 23
3.3.2. Assembly and validation of the high-throughput fluorescent enzyme-coupled activity assay 30
4. General conclusions 37
5. Acknowledgements 38
6. List of publications 39
7. References 41

Keywords: biocatalysis, non-natural amino acids, phenyalanine ammonia-lyases, ferulic acid decarboxylase, high-throughput enzyme activity methods

1. Introduction

1.1. Optically pure amino acids

Enantiopure non-natural amino acids (*ee* > 99%) are important building blocks for the synthesis of many pharmaceutical drugs, for the preparation of new cyclic and linear peptidic drugs[1] by their incorporation in non-ribosomal peptides (NRPs). L- and D-biarylalanines are important chiral building blocks for the preparation of several inhibitors and Active Pharmaceutical Ingredient (APIs), both with implications in drug development[2]. Highly enantiomerically enriched heterocyclic amino acids are also frequently involved for the preparation of helpful substances. D-arylalanines are important intermediates in the synthesis of antiviral drugs, such as Fosamprenavir and Saquinavir, or for the antineoplastic Clientide, antidiabetic Nateglinide and anticoagulant Melagatran. *Para*-substituted L-or D-phenylalanines with electron-withdrawing groups, like *fluoro-*, *chloro-* and *nitro-* are precursors of antiemetic Aprepitant, antineoplastic Abarelix and analgesic Zolmitriptan[3]. The incorporation of L-4-F-, 4-Br-, 4-Me- or 4-MeO-phenylalanines in various structures led to four new sansanmycin analogues, which are members of uridyl-peptide antibiotics (UPAs)[4] (**Figure 1.**).

The current thesis focuses on the use of phenylalanine ammonia-lyases (PALs), as useful biocatalysts for the production of optically pure D- and L-phenylalanine derivatives[5].

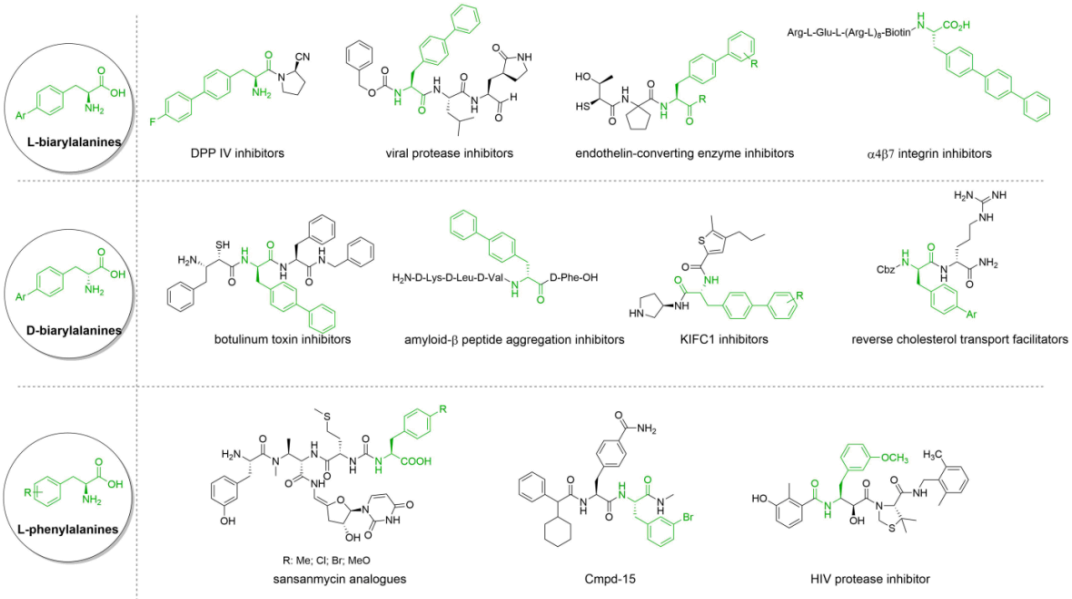

Figure 1. Optically pure non-natural amino acids as chiral building blocks

1.2. Phenylalanine ammonia lyase from *Petroselinum crispum* (*Pc*PAL)

Phenylalanine ammonia lyases (PALs) in the form of various isoenzymes are widely found in plants as well as in yeasts and fungi[6]. Due to the broad substrate tolerance, phenylalanine ammonia lyase from *Petroselinum crispum* (*Pc*PAL) is the most performant MIO-deppendent ammonia lyase.

*Pc*PAL can be used for the stereoselective synthesis of amino acids. Under natural reaction conditions, starting from racemic amino acids as substrates, by the L-selective ammonia elimination, the non-reactive D-amino acids can be obtained with a theoretical maximum yield of 50%. Contrary, in the presence of high ammonia concentration the same enzymes can mediate the reverse reaction, namely the ammonia addition onto α,β-unsaturated acrylic acids, yielding L-amino acids with a theoretical maximum yield of 100% (**Figure 2.**).

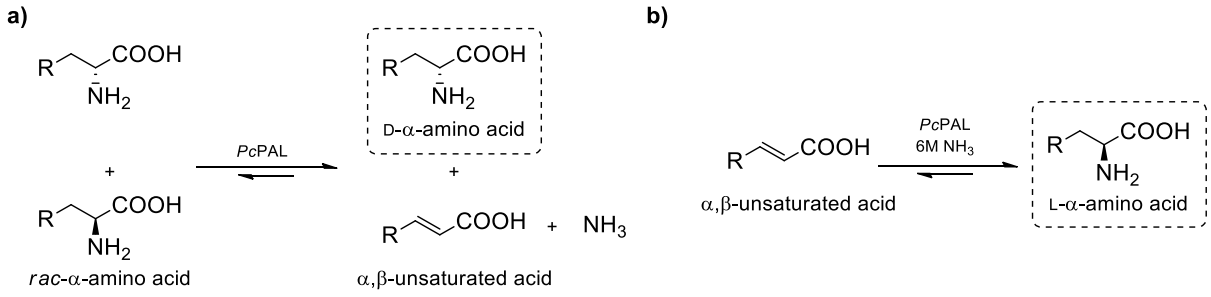

Figure 2. a) *Pc*PAL catalyzed stereoselective elimination with a maximal theoretical yield of 50%. **b)** *Pc*PAL catalyzed stereoselective addition with a maximal theoretical yield of 100%.

The active site of the *Pc*PAL enzyme contains a hydrophobic binding region (marked with purple) and a polar, carboxylic- and amine-binding region (marked with red), as well the MIO group (marked with green) (**Figure 3.**)[7].

Mutational studies in the carboxylic- and amino- group binding region in the active site of the enzyme revealed the essential amino acid side chains. Mutational studies were also performed in the hydrophobic binding region (marked with purple) of the enzyme which leads to increased enzyme activity in comparison with the *wild-type* enzyme. Mutation of the Phe137 residue to Val showed increased reaction rates in the deamination and amination reaction of the substrates L-Phe and L-p-NO_2-Phe[7].

However, it was still questionable if during the accommodation of substrates aryl moiety in the hydrophobic binding pocket of the catalytic site, is there any correlation

between the position (*ortho*-, *meta*-, *para*-) of the substrates aryl ring substituents and certain well defined specific amino acid residues of the protein.

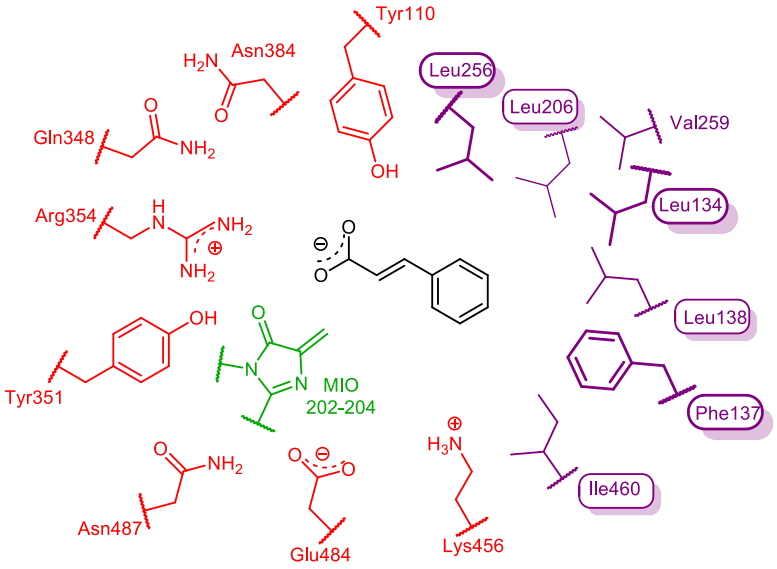

Figure 3. The active site of the *Pc*PAL enzyme according to active site model of *Pc*PAL (PDB ID 1W27) with modeled *trans*-cinnamic acid[8]

1.3. Coupling the PAL-catalyzed reactions with the FDC1-catalyzed decarboxylation

The cascade biotransformations are gaining ground in the last decade. The efficacy of coupling the PAL catalyzed transformations with other enzymatic reactions, such as the ferulic acid decarboxylase (FDC1) mediated decarboxylation have been demonstrated within for the production of several valuable fine chemicals using engineered whole-cell biocatalysts containing both *pal* and *fdc1* genes[9,10,11]. Primary studies focused on styrene production by the PAL-FDC1 tandem starting from L-phenylalanine biosynthesized by the same cell from glucose through an intensified shikimate pathway[12,13].

On the other hand, recent studies showed that diaryltetrazole can be employed for the high sensitivity in the detection of alkenes[14,15,16], generating fluorescent products through a photoactivated 1,3-dipolar cycloaddition. Moreover, the compatibility of the detection in case of biological systems was also demonstrated by the successful labeling of alkene-containing proteins in *E.coli*[16].

Aware of these we proposed the development of a novel high-throughput fluorescence enzyme-coupled activity assay for PAL-catalyzed reactions using ferulic acid decarboxylase (FDC1) to decarboxylate cinnamic acid, the product/substrate of the natural/reverse PAL-

reaction, followed by the cycloaddition reaction between the produced styrene and a tetrazole fluorogenic probe (**Figure 4.**).

Accordingly within the novel PAL-activity assay ferulic acid decarboxylase (FDC1) from *Saccharomyces cerevisiae* was envisaged to be employed as coupled-enzyme. Therefore the compatibility of the substrate scope, reaction condition of the two enzymes, *Pc*PAL and *Sc*FDC1 also had to be evaluated.

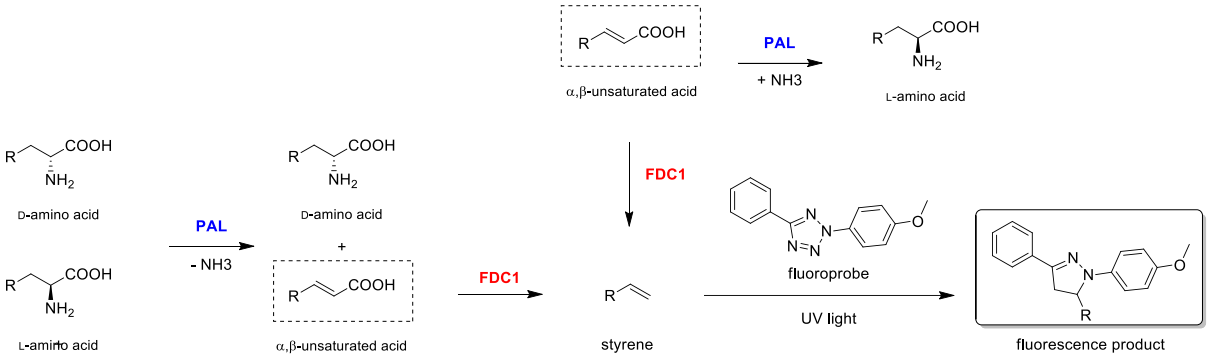

Figure 4. The proposed PAL and FDC1 coupled fluorescence assay

1.3.1. Ferulic acid decarboxylase (FDC1) from Saccharomyces cerevisiae

The decarboxylation reaction catalyzed by *Sc*FDC1 is the firstly discovered enzymatic reaction which involves an initial 1,3-dipolar cycloaddition between prFMN and the double bond of phenylacrylic acid[17].

- **Substrate scope**

The biocatalytic utility of this enzyme was demonstrated only on few *para*-substituted cinnamic acids as shown in **Figure 5**[17].

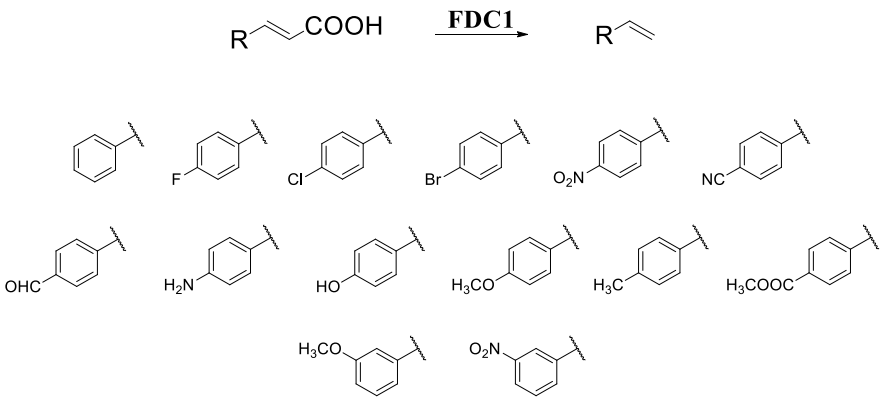

Figure 5. The *Sc*FDC1 enzyme studied substrate region

Nonetheless, the broader substrate scope of the *Sc*FDC1 enzyme was still unexplored. For the development of a trustful and versatile FDC1 assisted PAL-activity assay valid for a broad substrate range, proofing the overlap of the substrate domains of the two employed enzymes is mandatory.

2. Aims of the study

The main aim of the thesis is the ***development of engineered PAL biocatalysts useful for the synthesis of several highly valuable non-natural phenylalanine analogues***. To fulfill the targeted aim the successful outcomes of the following objectives have been envisaged:

Objective 1. Chemical synthesis of substrates and development of the analytical methods used for monitoring the enzymatic reactions. The synthesis of differently (*ortho*-, *meta*-, *para*-) substituted phenyl-, bulky heteroaryl- or biaryl-analogues of phenylalanine and cinnamic acid, serving as substrates for PAL reactions (Obj. 2., and 3.1.) and also for ferrulic acid decarboxylase mediated decarboxylations (Obj. 3.2.). For each enzymatic reactions HPLC methods for monitoring the enzyme activities through conversion determinations and/or stereoselectivity, through enantiomeric excess determinations, will be developed.

Objective 2. Rational design-based protein engineering of PAL from *Petroselinum crispum*. Based on existing structural information of PALs, we envisaged the mapping of the active site of *Pc*PAL through mutational analysis, in order to identify potential sterical correlations between the substituents attached in various position (*ortho*-, *meta*-, *para*-) to the aryl ring of the substrate and specific active site residues from the hydrophobic binding region of the enzyme (**Figure 6.**).

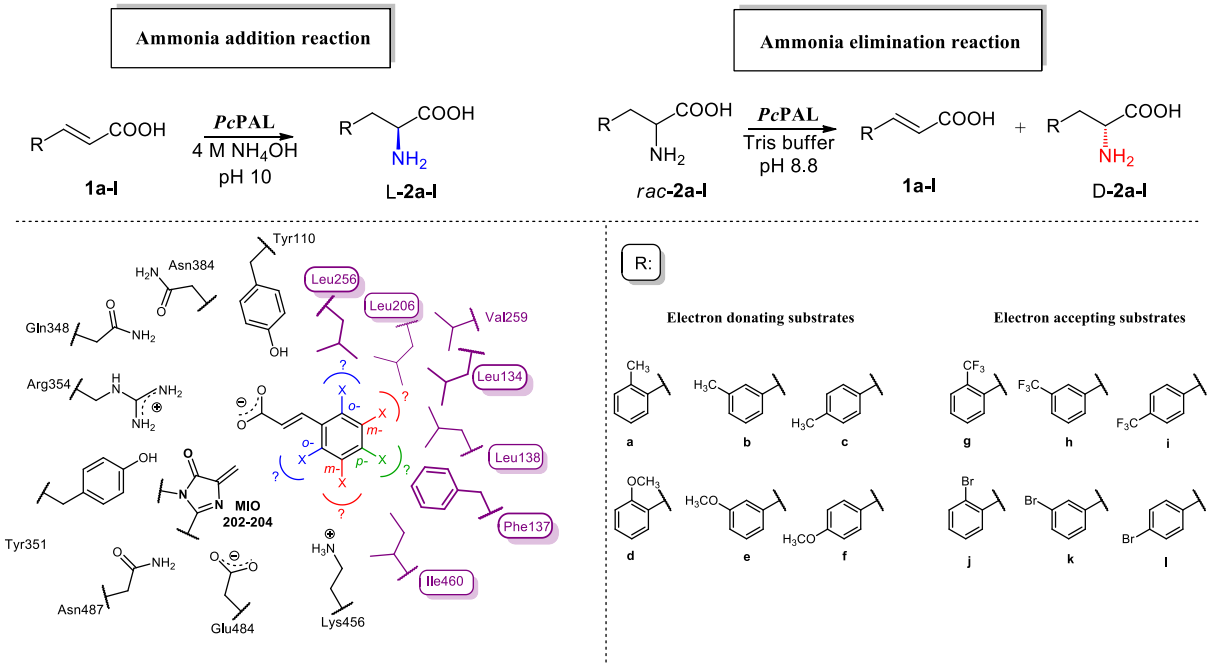

Figure 6. Rational redesign of the *Pc*PAL and its applicability for the synthesis of phenylalanine and cinnamic acid analogues of high synthetic value

Objective 3. Development of a novel high-throughput PAL-activity assay applicable for directed evolution based protein engineering. While high-throughput PAL-activity assays have been developed[16], their general applicability was still limited. Accordingly, we envisaged to develop an enzyme-coupled fluorescent assay applicable for PAL-activity screens at whole cell level, involving decarboxylation of *trans*-cinnamic acid (the product of the PAL reaction) by ferulic acid decarboxylase (FDC1) and a photochemical reaction of the produced styrene **3a'** with a diaryltetrazole **4**, that generates a detectable, fluorescent pyrazoline product **5** (**Figure 7.**).

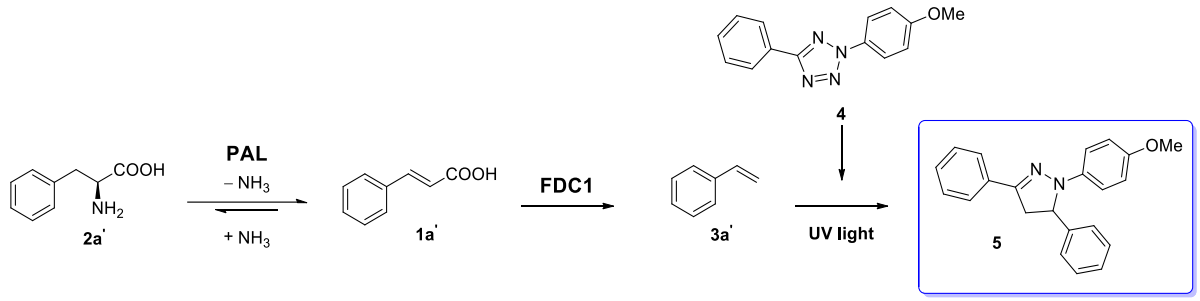

Figure 7. Proposed enzyme-coupled fluorescent assay applicable for PAL-activity screens

Objective 3.1. Exploring and extending the substrate scope of ferulic acid decarboxylase for ensuring its compatiblity with the substrate domain of PALs. The substrate scope of *Sc*FDC1 was tested using cinnamic acid analogues which can be obtained from the PAL-reactions. A broad substrate scope of ScFDC1 would provide general applicability of the enzyme-coupled assay towards PAL-activities for various substrates (**Figure 8.**).

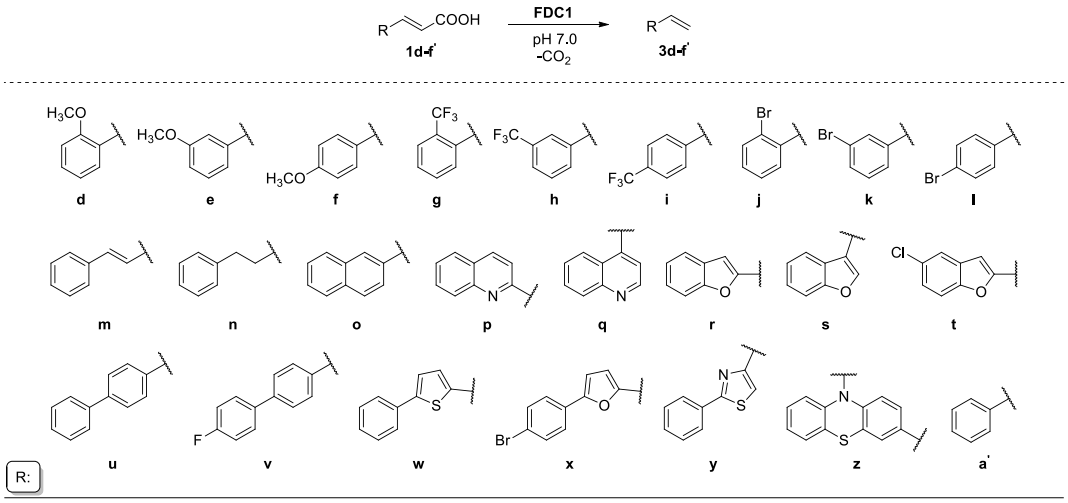

Figure 8. Exploring the substrate scope of *Sc*FDC1 using cinnamic acid analogues which can be obtained from the PAL-reactions

Objective 3.2. Assembly and validation of the high-throughput fluorescent enzyme-coupled activity assay for the natural PAL-reaction. The developed enzyme-couples assay was tested within the activity screens of large mutant libraries of PALs (obtained within *Objective1*) in presence of non-natural substrates of interest. Furthermore the general applicability of the fluorescent assay for PALs of different origin, as well as its versatility for the detection of tyrosine ammonia-lyase (TAL) activity was also studied.

3. Results and discussion

3.1. Chemical synthesis of substrates and development of the analytical methods used for monitoring the enzymatic reactions

3.1.1. Chemical synthesis of racemic amino acids *rac*-2a-l

The racemic amino acids *rac*-**2a-l** were obtained via a synthesis route starting from the commercially available aldehydes **6a-l**. The aldehydes **6a-l** were reduced to primary alcohols **7a-l** using $NaBH_4$. The primary alcohols **7a-l** were halogenated and from the brominated compounds **8a-l** *via* malonic acid coupling were obtained the diethyl acetamidomalonates **9a-l**. Through a mild alkaline hydrolysis of **9a-l**, followed by a decarboxylation reaction the *N*-acylated amino acids *rac*-**10a-l** were obtained. Finally, the racemic amino acids *rac*-**2a-l** were obtained by deprotection of *rac*-**10a-l** using acid hydrolysis (**Figure 9.**). The synthesized compounds *rac*-**2a-l** were characterized by ^1H and ^{13}C NMR measurements.

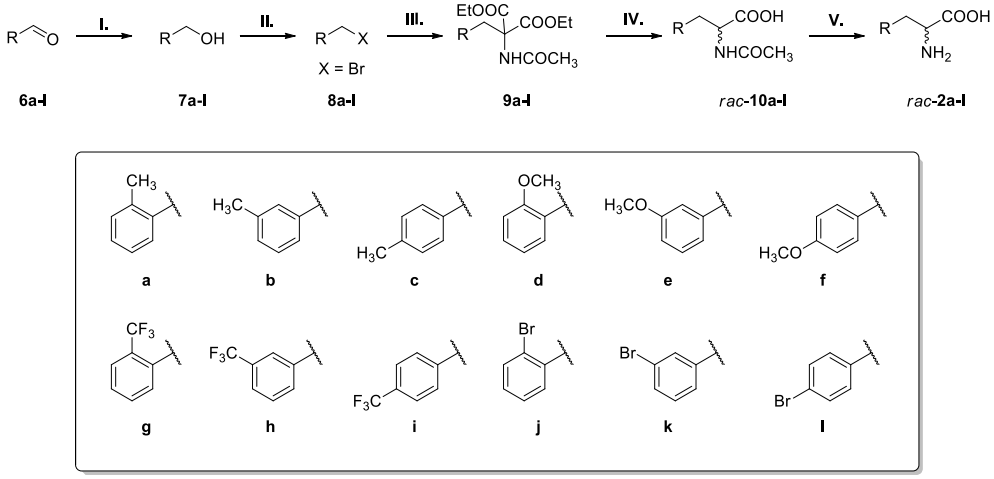

I. $NaBH_4$, MeOH, r.t; **II.** *N*-bromosuccinimide, PPh_3, CH_2Cl_2, r.t; **III.** NaH, $CH_3CONH(CO_2Et)_2$, DMF, 60°C; **IV.** a)10% NaOH, MeOH, reflux; b) toluene, reflux; **V.** 18% HCl, 1,4-dioxane, reflux

Figure 9. The synthesis of the racemic amino acids *rac*-**2a-l**

3.1.2. Chemical synthesis of acrylic acids

The synthesis of acrylic derivatives **1a-z, 1a'** was performed using the corresponding aldehydes **6a-a'** as starting material, with the Knoevenagel-Doebner reaction (**Figure 10.**). The synthesized compounds **1a-z, 1a'** were characterized by ^1H and ^{13}C NMR measurements.

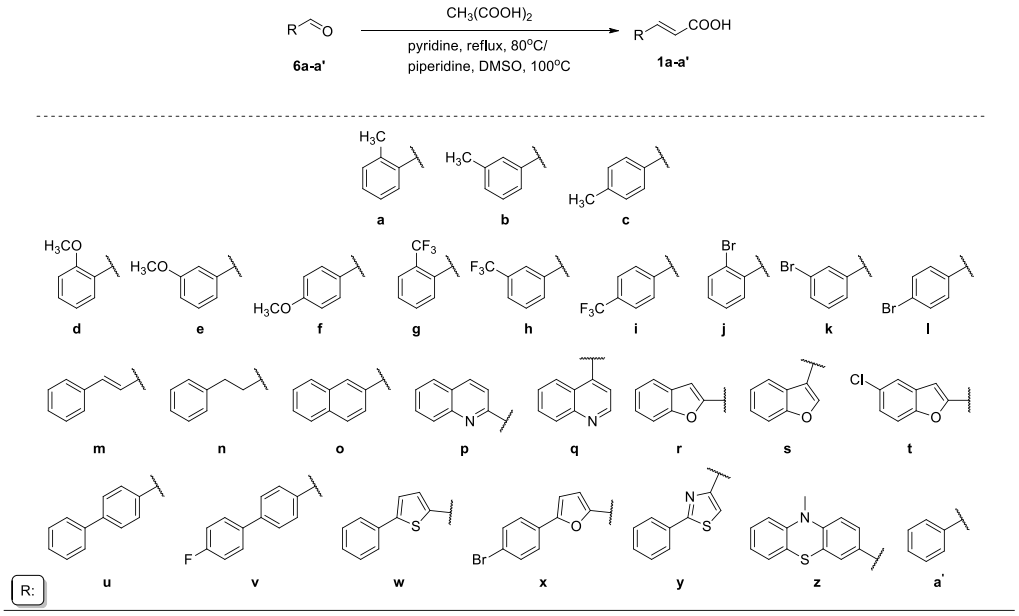

Figure 10. The synthesis of the acrylic acid derivatives **1a-z, 1a'**

3.1.3. Synthesis of the fluorogenic diaryltetrazole probe

The tetrazole fluorogenic probe **4**, useful for the development of the fluorescent PAL-activity assay (*Objective 3*), was obtained *via* a synthesis route starting from the commercially available aldehyde **6a'**. The aldehyde **6a'** in the reaction with phenylsulfonylhydrazine results the phenylsulfonylhydrazone **11**, which upon reaction with 4-methoxyphenyldiazonium salt **13** resulted the tetrazole product, 2-(4-methoxyphenyl)-5-phenyl-2*H*-tetrazole **4** (**Figure 11.**). The tetrazole derivative **4** was further used as fluorogenic probe within the fluorescent assay.

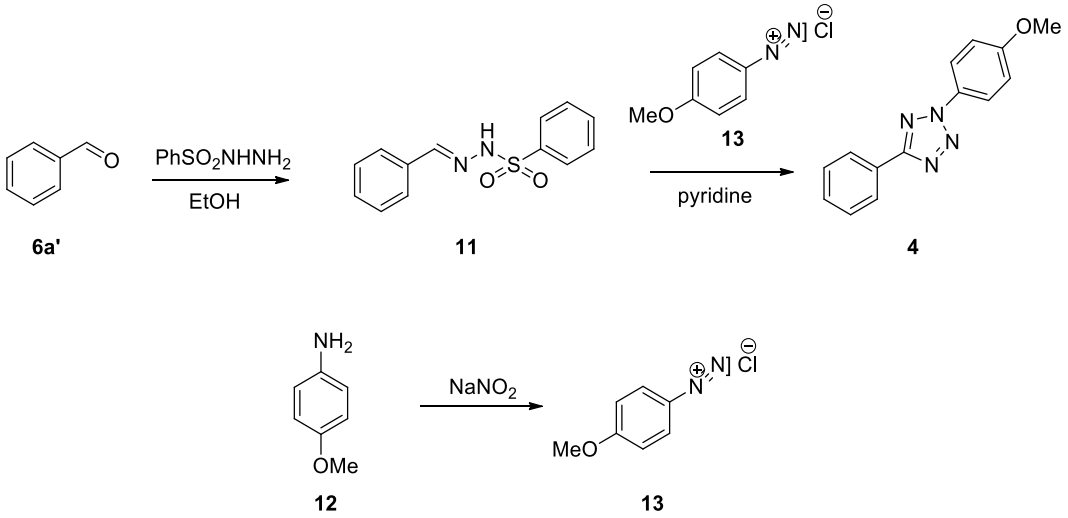

Figure 11. Synthetic route for 2-(4-methoxyphenyl)-5-phenyl-2*H*-tetrazole (**4**)

3.1.4. HPLC methods for the conversion determination of PAL-mediated biotransformations

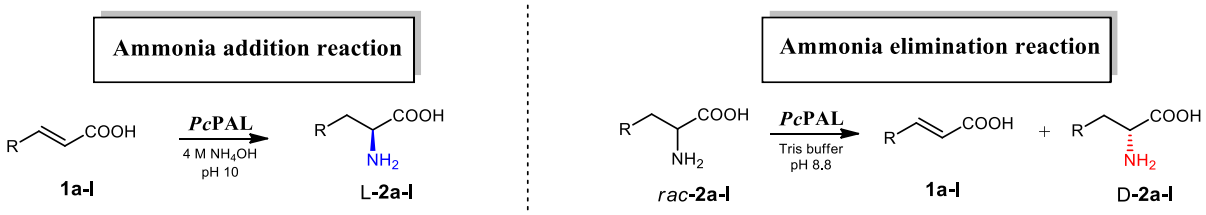

Figure 12. *Pc*PAL-catalyzed ammonia addition and ammonia elimination reactions

To investigate the conversions of the *Pc*PAL-catalyzed ammonia elimination and ammonia addition reactions (**Figure 12.**), the relative response factor of the product and substrate, the cinnamic acid derivatives reported to the amino acids have been determined. For this purpose the mixture of known composition of the corresponding racemic amino acid *rac*-**2a-l** and the corresponding acrylic derivative **1a-l** was injected onto Gemini NX-C18 column (150 × 4.5 mm; 5 µm) and eluted with different conditions (ensuring baseline separation of the racemic phenylalanine and the corresponding cinnamic acid derivatives), while the ratios of the corresponding peak areas were correlated to the molar ratios of the reactant and product.

To determine the enantiomeric excess (*ee*) value of D-**2a-l** obtained from the ammonia elimination reactions and L-**2a-l**, product of the ammonia addition reactions, chiral HPLC separation methods of the *rac*-**2a-l** have been developed using Crownpak CR-I (+) chiral column (150 × 3 mm; 5 µm) and $HClO_4$ (pH=1.5): ACN as mobile phase, at different flow rate.

3.1.5. HPLC methods for the conversion determination of FDC1-mediated biotransformations

To explore the substrate scope of *Sc*FDC1 (Objective 3.1), HPLC methods for conversion determinations of the FDC1 catalyzed enzymatic reactions were developed. Quantification of the conversions were based on the consumption of the cinnamic acid substrates **1d-z, a'**, monitored by RP-HPLC, using anisol as internal standard and Gemini NX-C18 150x4.5 mm or Zorbax SB-C8 50x2.1 mm columns, at flow rate: 1mL/min under different elution conditions. Calibration curves were obtained by injecting mixtures of different concentration of cinnamic acid derivatives and fixed (5 mM) concentration of internal standard.

3.2. Rational design-based protein engineering of PAL from *Petroselinum crispum*

3.2.1. Generating a library of *Pc*PAL single mutants through rational design

By the individual replacement through site-directed mutagenesis of each residue from the hydrophobic binding pocket of the *Pc*PAL active site to less voluminous Ala (**A**) and Val (**V**), a concise library of single mutants was obtained (**Figure 13.**).

Entry	*Pc*PAL mutants
1	**L134A**
2	**L134V**
3	**F137A**
4	**F137V**
5	**L138A**
6	**L138V**
7	**L206A**
8	**L206V**
9	**L256A**
10	**L256V**
11	**I460A**
12	**I460V**

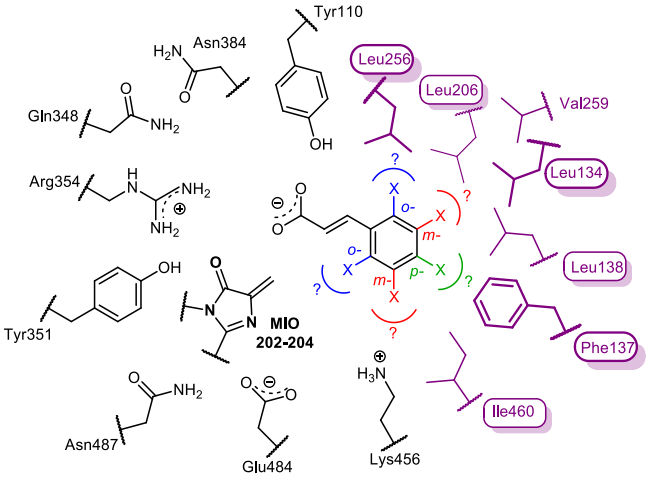

Figure 13. List of the *Pc*PAL single mutant library, obtained by replacing the residues of the hydrophobic binding pocket (purple) of the enzyme active site to less voluminous Ala (**A**) and Val (**V**)

3.2.2. Screening the activity and selectivity of the *Pc*PAL-mutant library

We tested the *Pc*PAL-single mutant library in the ammonia addition and ammonia elimination reactions, using as substrates cinnamic acid and phenylalanine analogues, mono-substituted at all positions (*o*-, *m*-, *p*-) of the aromatic ring with both electron-donating (-CH_3, -OCH_3) and electron-withdrawing (–CF_3, -Br) substituents (**Figure 14.**). First relative initial enzyme activities were measured in order to identify the best mutant variants with the highest enzyme activities both in the ammonia elimination and addition reactions (**Figure 15., Figure 16.**). The best performing mutants with the three highest conversions and relative activities were further used in selectivity screens, and besides the conversion values of substrates, the enantiomeric excesses (ee_p) of products were also determined (**Table 1-3.**).

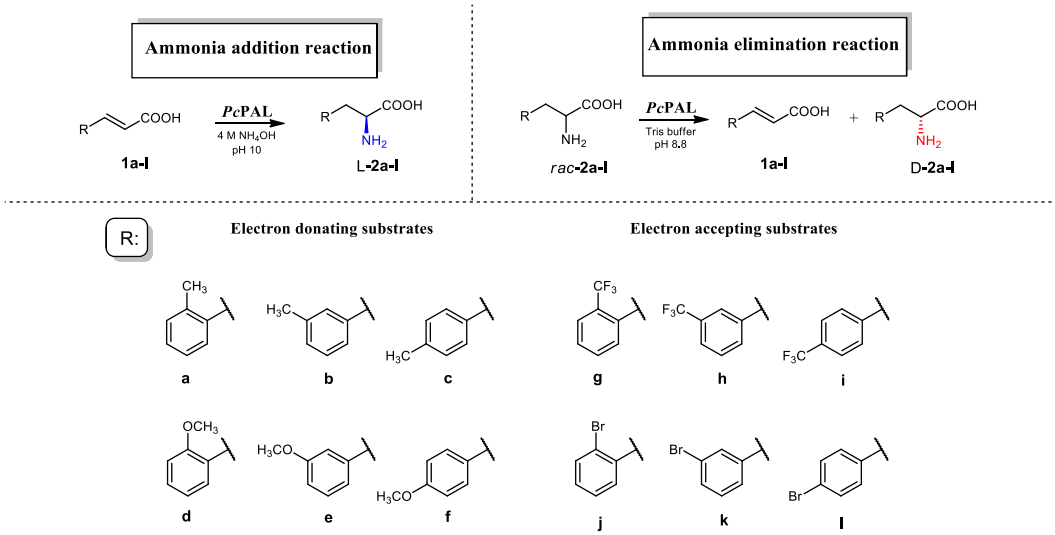

Figure 14. Cinnamic acid and phenylalanine analogues, mono-substituted at all positions (*o*-, *m*-, *p*-) with electron-donating (-CH_3, -OCH_3) and electron-withdrawing (–CF_3, -Br) substituents used in the ammonia addition and elimination reaction of the *Pc*PAL single mutants

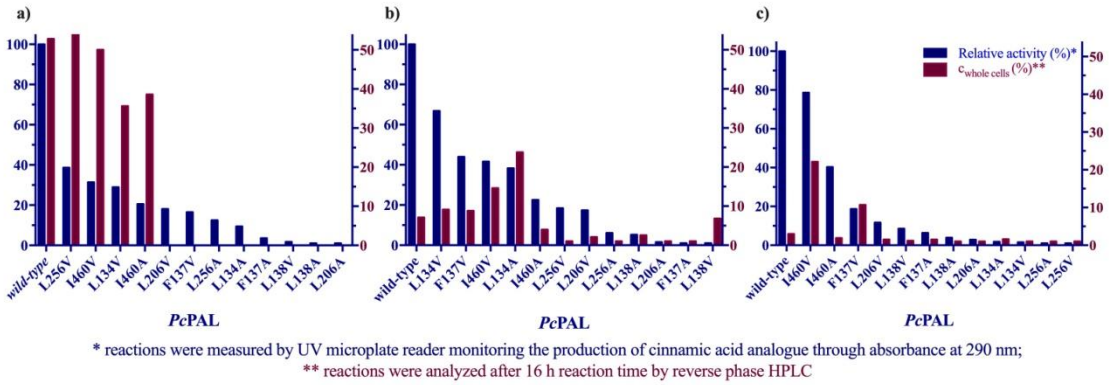

Figure 15. Representative activity screening for the ammonia elimination reactions of the methyl-susbstituted phenylalanine analogues *rac*-**2a**, **2b**, **2c**

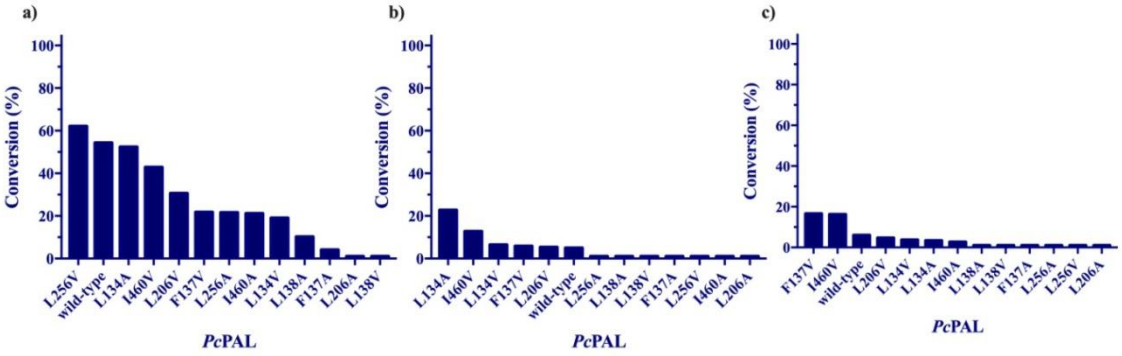

Figure 16. Conversion values of ammonia addition reactions of methyl-susbstituted acrylic acid derivatives **1a**, **1b**, **1c** after 16 h

The best performing mutants with the three highest conversions and relative activities were further used in selectivity screens, and besides the conversion values of substrates, the enantiomeric excesses (ee_p) of products were also determined (**Table 1-3.**).

Both in ammonia addition and elimination reactions similar mutations provided enhanced catalytic properties, despite the differences between the reaction medium of the ammonia addition (4−6 M NH_3, pH 10, buffered with CO_2) and ammonia elimination (Tris.HCl, pH 8.8) reactions, suggesting that the hydrophobic pocket of the active site adopts similar fold relative to the substrate in both reaction routes.

In case of *o*-substituted substrate analogues wt-*Pc*PAL and L256 variant provided highest conversions both in ammonia addition and elimination reactions, excepting in case of *o*-methoxy substituted substrates *rac*-**2d** and **1d** where the mutants L256 and *wild-type Pc*PALs provided low activity (0-1% conversion), while mutant L134A, similarly as in case of substrates containing linear *meta*-substituents (**1b,e,k,***rac*-**2b,e,k**), showed significantly increased conversion (29.3% for *rac*-**2d** and 47.9% for **1d**), supporting a spatial orientation of the methyl group towards of residue L134 (**Table 1.**).

Tabel 1. Conversion and enantiomeric excess values of the best *Pc*PAL single mutants and *wild-type Pc*PAL in the ammonia addition and elimination reactions on *ortho*-substituted substrates after 16 h reaction time

	ortho-substituent	Electronwithdrawing group						Electrondonor group					
		-Br			-CF_3			-CH_3			-OCH_3		
		E	c (%)	ee (%)	E	c (%)	ee (%)	E	c (%)	ee (%)	E	c (%)	ee (%)
Reaction type	Ammonia addition*		**1j**			**1g**			**1a**			**1d**	
		L256V	91.5	>99	L134A	78.4	>99	L256V	62.1	>99	L134A	47.9	>99
		L256A	89.8	>99	L256V	77.6	>99	wt	54.3	>99	L134V	18.5	>99
		wt	89.0	>99	wt	76.2	>99	L134A	52.4	>99	L206V	5.7	>99
		F137V	85.9	>99	L206V	76.1	>99	I460V	47.4	>99	wt	<1	-
	Ammonia elimination*		*rac*-**2j**			*rac*-**2g**			*rac*-**2a**			*rac*-**2d**	
		L256V	49.1	97.2	L256V	50.8	>99	L256V	54.9	>99	L134A	29.3	41.1
		L256A	44.8	84.8	L206V	51.8	>99	wt	52.8	>99	I460V	1.3	1.3
		I460V	44.7	79.3	L256A	50.0	>99	I460V	50	>99	wt	1.0	1.1
		wt	42.0	72.4	wt	49.0	94.0	I460A	38.6	62.8	L256A	<1	-

*the reactions were performed under the conditions of the initial screenings

In case of *meta*-substituted substrates mutations of L134A and I460V provided higher conversions both in ammonia addition and elimination reactions (**Table 2.**), in accordance with the proposed substrate binding model (**Figure 13.**), since mutation of both L134, I460 residues to less voluminous Ala (**A**) and Val (**V**) could provide more space for the *meta*-substituents of the substrate.

Tabel 2. Conversion and enantiomeric excess values of the best *Pc*PAL single mutants and *wild-type* *Pc*PAL in the ammonia addition and elimination reactions on *meta*-substituted substrates after 16 h reaction time

	meta-substituent	Electronwithdrawing group						Electrondonor group					
		-Br			-CF_3			-CH_3			-OCH_3		
		E	c (%)	ee (%)	E	c (%)	ee (%)	E	c (%)	ee (%)	E	c (%)	ee (%)
Reaction type	Ammonia addition*		**1k**			**1h**			**1b**			**1e**	
		L134A	79.6	>99	I460V	36.9	>99	L134A	22.7	>99	L134A	73.0	>99
		I460V	68	>99	L134A	17.5	>99	I460V	12.7	>99	F137V	24.5	>99
		I460A	29.6	>99	L138V	11.1	>99	L134V	9.8	>99	wt	16.9	>99
		wt	28.9	>99	wt	<1	-	wt	4.9	>99	I460V	4.2	>99
	Ammonia elimination*		*rac*-**2k**			*rac*-**2h**			*rac*-**2b**			*rac*-**2e**	
		L134A	48.9	94.1	I460V	31.4	49.5	L134A	23.8	31.2	L134A	51.2	>99
		I460V	42.4	77.8	L134A	26.2	38.5	I460V	14.6	20.4	L134V	29.5	40.3
		wt	31.4	47.0	wt	9.1	9.9	L134V	9.1	10.2	wt	16.1	20.2
		F137V	24.5	33.0	F137V	6.9	7.5	wt	7.1	7.7	I460V	7.9	8.7

*the reactions were performed under the conditions of the initial screenings

Expectedly, low conversions were obtained with *wt-Pc*PAL in case of *para*-substituted substrates (except the moderate conversion of 34.2% for *p*-bromo-substituted *rac*-**2l**), and the mutants F137V and I460V provided higher activity. For some substrates like **1l** and **1i**, the conversions with F137V variant were higher (c=61.2% for **1l** and c=73.9% for **1i**) than those with I460V mutant (c=51.1% for **1l** and c=20.4% for **1i**), but the enantioselectivity was higher for I460V ($ee_{L\text{-}2i}$ and $ee_{L\text{-}2l}$ of 99% when using I460V, $ee_{L\text{-}2i}$=97% and $ee_{L\text{-}2l}$=91.0% when using F137V) (**Table 3.**).

Tabel 3. Conversion and enantiomeric excess values of the best *Pc*PAL single mutants and *wild-type Pc*PAL in the ammonia addition and elimination reactions on *para* substituted substrates after 16 h reaction time

	para-substituent	Electronwithdrawing group						Electrondonor group					
		-Br			-CF_3			-CH_3			-OCH_3		
		E	c (%)	ee (%)	E	c (%)	ee (%)	E	c (%)	ee (%)	E	c (%)	ee (%)
Reaction type	Ammonia addition*	**1l**			**1i**			**1c**			**1f**		
		F137V	61.2	97	F137V	73.9	91.0	F137V	16.6	>99	I460V	11.8	>99
		I460V	51.1	>99	I460V	20.4	>99	I460V	16.2	>99	F137V	5.4	>99
		L138V	13.2	>99	F137A	16.6	>99	wt	6.0	>99	L138A	2.9	>99
		wt	7.6	>99	wt	5.7	>99	L134V	3.7	>99	wt	<1	-
	Ammonia elimination*	*rac*-**2l**			*rac*-**2i**			*rac*-**2c**			*rac*-**2f**		
		I460V	49.8	>99	F137V	48.8	81.5	I460V	22.1	25.8	F137V	21	26.1
		F137V	45.0	95.9	I460V	36	51.7	F137V	10.7	23.8	I460V	16.8	19.1
		wt	34.2	54.3	F137A	30.1	42.2	wt	3.0	3.1	I460A	12.0	15.1
		L256V	7.9	8.6	wt	5.9	6.3	I460A	1.9	1.9	wt	<1	-

*the reactions were performed under the conditions of the initial screenings

3.2.3. Enzyme kinetic measurements

Further, enzyme kinetic parameters such as Michaelis contanst (K_M) *turnover number* (k_{cat}), *specificity constant* (k_{cat}/K_M) were determined using as model substrates *o*-, *m*-, *p*-CF_3-phenylalanines (*rac*-2g,h,i) the purified *wild-type Pc*PAL and the best-performing variants as biocatalysts within the ammonia elimination reactions (**Table 4.**).

Table 4. Kinetic parameters for the ammonia elimination reactions of *rac*-**2g,h,i**

***Pc*PAL**	***rac*-2g (*o*-CF_3)**			***rac*-2h (*m*-CF_3)**			***rac*-2i (*p*-CF_3)**		
	wt	**L206V**	**L256V**	**wt**	**I460V**	**L134V**	**wt**	**F137V**	**I460V**
K_M (µM)	523	743	2733	533	163	912	2490	151	901
k_{cat} (s^{-1})	0.042	0.041	0.148	0.057	0.200	0.203	0.25	0.42	0.55
k_{cat}/K_M (s^{-1} M^{-1})	61.7	64.8	54.2	103.2	1227.0	222.8	100.4	2781.4	611.1

In accordance with the conversion value-based ranking of the mutant variants, obtained with whole cells PAL-biocatalysts, the k_{cat} values obtained with purified enzyme, were also significantly higher for the best-performing mutants than those for the wt-*Pc*PAL. The higher K_M values in the case of *o*- and *m*-CF_3-phenylalanines (*rac*-**2g,h**), suggest lower affinity and is in accordance with previous studies[18], where a more relaxed arrangement of the substrate within the catalytic site for the tested mutant variants was suggested. As exception, for the *m*-CF_3-phenylalanine (*rac*-**2h**) the I460V mutant shows increased activity and also affinity and supports the proposed interaction of the electron-withdrawing substituents with residue K456 (**Figure 13.**). The k_{cat}/K_M values increased in the case of the best performing mutants for the model substrates in kinetic measurements in comparison with the k_{cat}/K_M values for the wt-*Pc*PAL (**Table 4.**), supporting the increased catalytic efficiency observed also within the whole-cell biotransformation.

3.2.4. Synthetic aplicability of the engineered *Pc*PAL variants.

The preparative scale biotransformations were performed on 500 mg scale. The enantiopure phenylalanine analogous (*S*)-2k and (*R*)-2c were isolated using ion-exchange chromatography with high yields: 94% and 60%. The optical purity of the products were: $ee_{(S)\text{-}2k}$> 99% and $ee_{(R)\text{-}2c}$= 97% (**Figure 17**.).

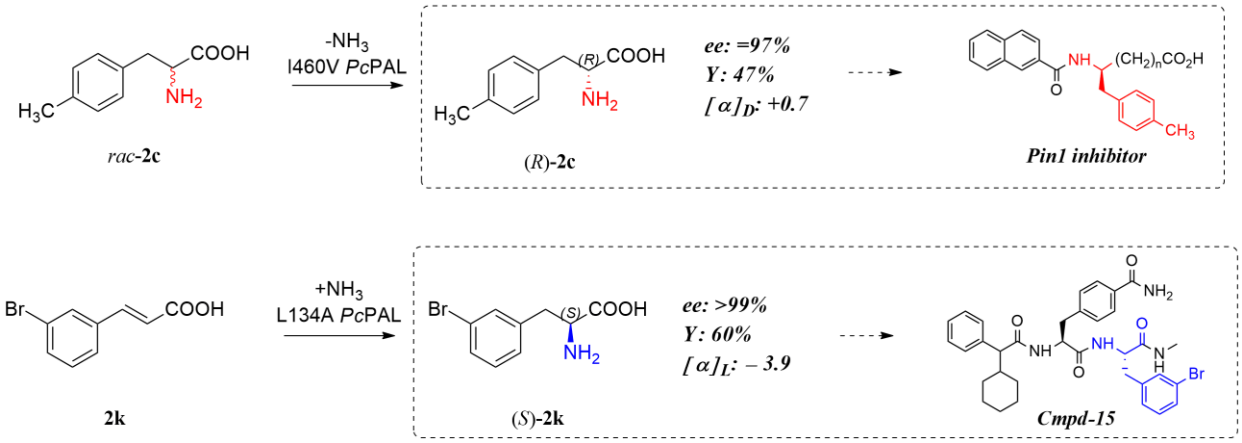

Figure 17. The preparative scale biotransformations for the ammonia addition reactions of *m*-bromo-cinnamic acid **1k** using L134A *Pc*PAL and for the ammonia elimination reactions of racemic *p*-methyl-phenylalanine *rac*-**2c** using I460V *Pc*PAL

3.2.5. Crystallization studies

Crystallization studies were also performed to further support the orientation of the differently positioned of (*ortho*-, *meta*-, *para*-) substituents of the substrate aryl ring within the hydrophobic part of the active site of *Pc*PAL (**Figure 13.**) provided by the mutational analysis. The sample of the purified I460V *Pc*PAL variant the *p*-MeO cinnamic acid were prepared within the Biocatalysis and Biotransformation Research Center, while crystallization studies was performed by the collaborator group of Prof. Cristopher Schofield from the University of Oxford, Department of Chemistry, Chemistry Research Laboratory. The resulted crystal structure shows the I460V mutant of *Pc*PAL with the substrate *p*-methoxy cinnamic acid **1f** in the active site (**Figure 18.**) and has been deposited within the Protein Data Bank (PDB ID: 6RGS).

The active site residues of the crystallographic structure are in accordance with our model obtained from the mutational analysis. Analyses of the substrate binding mode shows the *para*-position of the aromatic ring in close proximity of the substituted residue 460. An overlay with the reported structure of the wt-*Pc*PAL[19] reveals a potential steric clash with the I460 side chain (**Figure 18.**). The other residues in the hydrophobic active site are in very similar positions as in our model (**Figure 18.**). An exception is the K456 which is between the F137 and I460 residues.

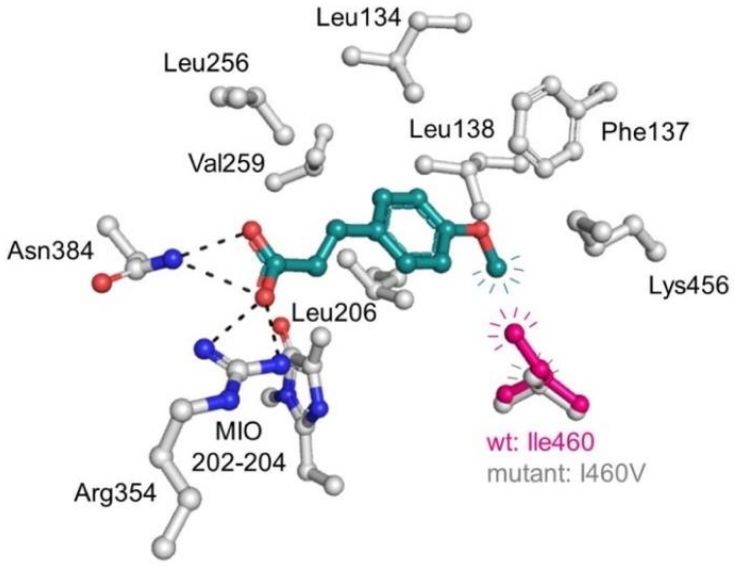

Figure 18. The crystal structure of the *Pc*PAL I460V mutant (PDB ID 6RGS) (I460 side chain is magenta) overlaid with the wt-*Pc*PAL (I60 side chain is gray) with the *p*-methoxy-cinnamic acid **1f** at the active site

3.2.6. Conclusions

It was revealed the correlation between the position (*ortho-*, *meta-*, *para-*) of the substrate's aryl ring substituent and specific active site residues within the hydrophobic binding region of the *Pc*PAL enzyme. Initially using the synthesized phenylalanine and cinnamic acid analogues, mono-substituted at all positions (*ortho-*, *meta-*, *para-*) of the aromatic ring with electron-donating (-CH_3, -OCH_3) and electron-withdrawing (-CF_3, -Br) substituents, we monitored the PAL mediated biotransformations in both reaction directions of ammonia eliminations and ammonia addition. The enzyme activity rankings obtained from conversion values of whole-cell biotransformations, were further supported by the kinetic parameters (K_M, k_{cat}, k_{cat}/K_M) obtained with purified enzyme biocatalysts. In accordance with the model created from the mutational strategy, the crystallographic analysis of the binding mode of *p*-methoxy cinnamic acid, at the active site of *Pc*PAL I460V, supports the proposed orientation of the methoxy group toward residue 460V and provides the first structure of an active PAL with a ring-substituted substrate analogue bound at the active site (PDB ID: 6RGS).

To demonstrate the synthetic applicability of the engineered *Pc*PAL variants, the preparative scale production of enantiopure phenylalanine analogues of high synthetic value, such as(*S*)-*m*-bromo-phenylalanine (*S*)-**2k** and (*R*)-*p*-methyl-phenylalanine (*R*)-**2c**, were obtained with high yields.

Accordingly we demonstrated that our rational design approach of PAL from *Petroselinum crispum* is highly efficient in providing PAL variant with significantly increased catalytic efficiency for the production of synthetically valuable phenylalanine analogues.

3.3. Development of high-throughput PAL-activity assay applicable for directed evolution based protein engineering

Directed evolution driven protein engineering is the most efficient procedure for expanding the substrate scope of enzymes, and/or to increase their catalytic activity[20,21,22]. However largely sized mutant libraries (>10^3-10^4 clones) are generated, from which the proper selection of hits have to be performed through high-throughput activity assays. While high-throughput PAL-activity assays have been developed[16], their general applicability is still limited.

In our aim to develop an enzyme-coupled assay for measuring the PAL-activity employing ferulic acid decarboxylase (FDC1) as coupled enzyme, first it was crucial to investigate the compatibility of the substrate scope of FDC1 and PAL enzymes.

3.3.1. Exploring and extending the substrate scope of ferulic acid decarboxylase for ensuring compatibility with the substrate domain of PALs

To explore the substrate scope of *Sc*FDC1, first the decarboxylation activity of the enzyme was tested using a largely sized substrate library (**Figure 19.**), containing cinnamic acid derivatives, which can be produced by the PAL-catalyzed ammonia eliminations of the corresponding phenylalanine analogues. The results showed that FDC1 transformed efficiently a wide variety of cinnamic acid analogues (**Table 5.**).

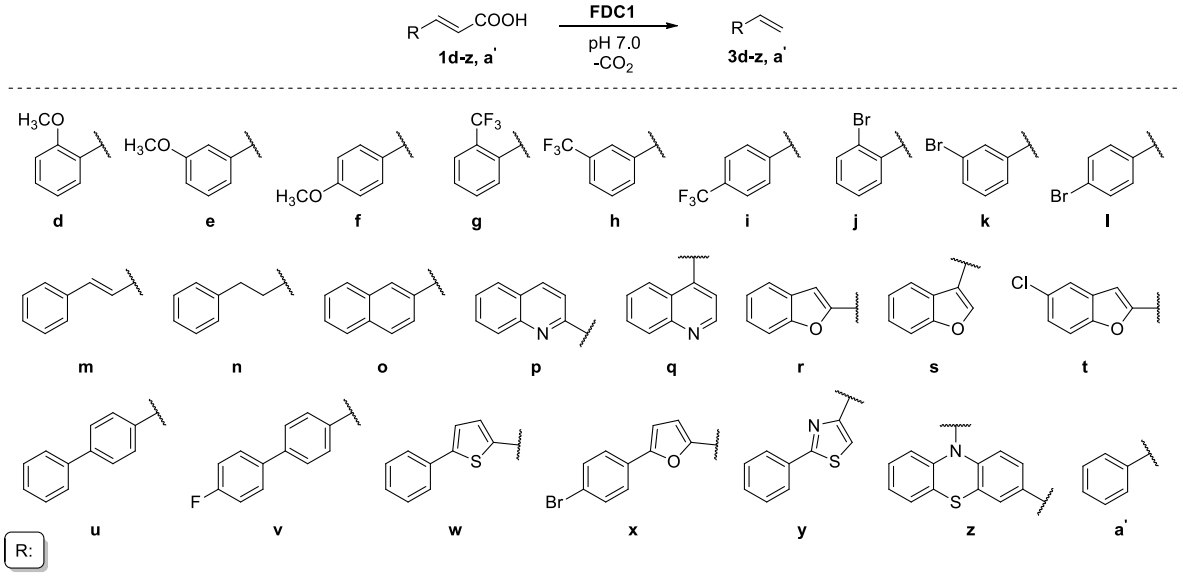

Figure 19. The FDC1 catalyzed decarboxylation reaction of cinnamic acid analogues **1d-z, a'**

Table 5. *Sc*FDC1-containing whole-cell biotransformations of **1d-a'**: **A)** conversions from initial screening, after 24 h reaction time **B)** maximal conversions obtained under optimized conditions: 100 mM sodium phosphate buffer pH 7.0, cells OD_{600} of ~1, 35°C.

Substrate		A	B	
		c* (%)	t (h)	c* (%)
(*E*)-3-(2-methoxyphenyl)acrylic acid	**1d**	82	48	92[a]
(*E*)-3-(3-methoxyphenyl)acrylic acid	**1e**	92	48	>99
(*E*)-3-(4-methoxyphenyl)acrylic acid	**1f**	86	72	>99
(*E*)-3-(2-(trifluoromethyl)phenyl)acrylic acid	**1g**	42	72	62[a]
(*E*)-3-(3-(trifluoromethyl)phenyl)acrylic acid	**1h**	80	48	87[a]
(*E*)-3-(4-(trifluoromethyl)phenyl)acrylic acid	**1i**	69	48	82[a]
(*E*)-3-(2-bromophenyl)acrylic acid	**1j**	80	48	83[a]
(*E*)-3-(3-bromophenyl)acrylic acid	**1k**	>99	8	>99
(*E*)-3-(4-bromophenyl)acrylic acid	**1l**	>99	24	>99
(2*E*,4*E*)-5-phenylpenta-2,4-dienoic acid	**1m**	95	48	>99
(*E*)-5-phenylpent-2-enoic acid	**1n**	<1	72	<1
(*E*)-3-(naphthalen-2-yl)acrylic acid	**1o**	96	48	>99
(*E*)-3-(quinolin-2-yl)acrylic acid	**1p**	31	8	39[b]
(*E*)-3-(quinolin-4-yl)acrylic acid	**1q**	33	8	28[b]
(*E*)-3-(benzofuran-2-yl)acrylic acid	**1r**	>99	8	>99
(*E*)-3-(benzofuran-3-yl)acrylic acid	**1s**	75	30	79[a]
(*E*)-3-(5-chlorobenzofuran-2-yl)acrylic acid	**1t**	93	8	>99
(*E*)-3-([1,1'-biphenyl]-4-yl)acrylic acid	**1u**	26	30	59[a]
(*E*)-3-(4'-fluoro-[1,1'-biphenyl]-4-yl)acrylic acid	**1v**	48	48	70[a]
(*E*)-3-(5-phenylthiophen-2-yl)acrylic acid	**1w**	82	72	85[a]
(*E*)-3-(5-(4-bromophenyl)furan-2-yl)acrylic acid	**1x**	<1	72	<1
(*E*)-3-(2-phenylthiazol-4-yl)acrylic acid	**1y**	<1	72	<1
(*E*)-3-(10-methyl-10H-phenothiazin-2-yl)acrylic acid	**1z**	<1	72	<1
cinnamic acid	**1a'**	75	24	>99

[a]-complete conversion reached after additional 24 h with fresh cell batch; [b]-no conversion increase after additional 24 h reaction time with fresh cell batch; *Determined through HPLC monitoring the substrate depletion.

3.3.1.1. Optimization of reaction conditions of the FDC1-mediated biotransformations

After the initial screenings the optimization of the whole-cell *Sc*FDC1 biotransformations were performed. The optimization consisted of the following: the effect of pH, temperature and biocatalysts/substrate ratio on the conversion values of the whole-cell biotransformations, using as model substrate 3-(3-(trifluoromethyl)phenyl)acrylic acid (**1h**).

The effect of pH on biotransformations

The influence of pH (6.0, 6.5, 7.0, 7.5, 8.0) on the FDC1-catalyzed decarboxylation reaction was tested with 3-(3-(trifluoromethyl)phenyl)acrylic acid (**1h**) using 100 mM sodium

phosphate buffer at pH 6.0, 6.5, 7.0, 7.5, 8.0. The highest conversion values were obtained at pH values of 6.0-7.0 (**Figure 20.**), in accordance with the reported pH optimum for the purified FDC1 enzyme[23].

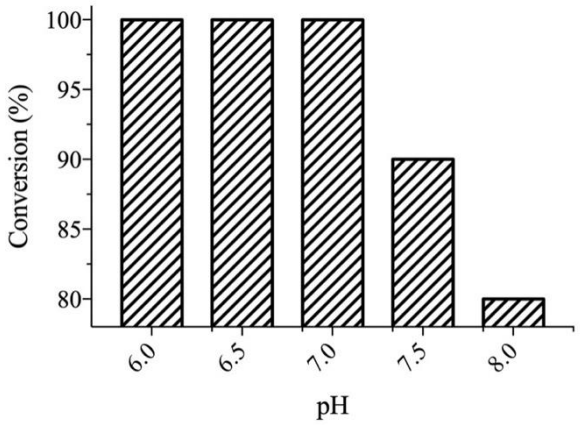

Figure 20. The effect of pH to the FDC1 catalyzed decarboxylation of **1h**

The effect of temperature on biotransformations

The influence of temperature (30, 35, 40, 45°C) on the FDC1-catalyzed decarboxylation reaction was tested with 3-(3-(trifluoromethyl)phenyl)acrylic acid (**1h**). The highest conversion values were obtained at 35°C (**Figure 21.**).

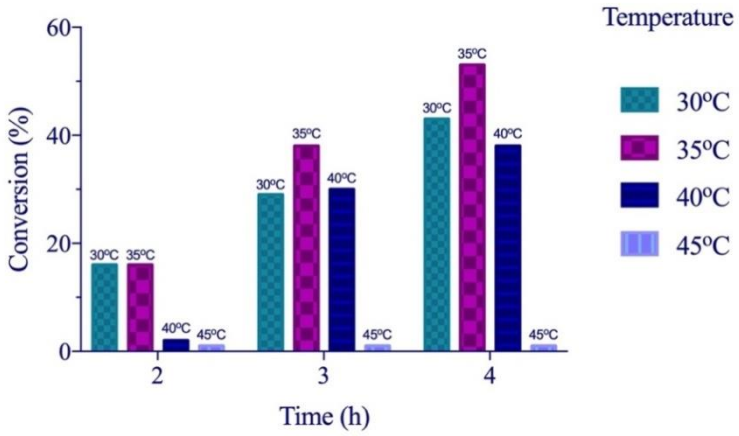

Figure 21. The effect of temperature on FDC1 catalyzed decarboxylation of **1h**

Effect of cells quantity on biotransformation

Further, the effect of biocatalyst/substrate ratio on conversion values was tested with 3-(3-(trifluoromethyl)phenyl)acrylic acid (1h) by using different amounts of whole-cell biocatalysts (OD_{600} of 1,2 or 3).

Increasing the amount of whole-cell biocatalyst, higher conversion was achieved after the same reaction time. Using cell density of OD_{600}=1 providing 42% conversion, whereas using higher cell densities of 2 and 3 conversion of 76% and complete conversion, respectively, were registered after 4 h reaction time. To avoid too short reaction times, which would disturb the precision of time-monitoring of the reaction, in further experiments, comparison of the *Sc*FDC1 activity with different substrates was performed at moderate cell densities (OD_{600} ≤2).

Time conversion profile of the FDC1-mediated biotransformations performed with the optimized procedure

Finally, to realize time conversion profiles, the *Sc*FDC1-catalyzed enzymatic reactions were performed under the optimal reaction conditions (100 mM sodium phosphate buffer pH 7.0, cells OD_{600} of ~1, 35°C) for the entire substrate panel (**1d-a'**) and the conversion values were monitored over longer time period (**Figure 22a,b.; Figure 23a,b.**), and the samples were taken after 1, 2, 3, 4, 8, 24, 30, 48, and 72 hours.

The decarboxylation reactions using the optimized reaction conditions of the whole-cell FDC1 reached complete conversions in the case of substrates **1a'**,**k**,**l**,**r**,**t** in relatively short reaction time (<24h, **Figure 22a.**, **Table 5B.**). For the substrates **1e**,**f**,**m**,**o** the conversions completed in longer reaction time (<72h, **Figure 22b.**, **Table 5B.**).

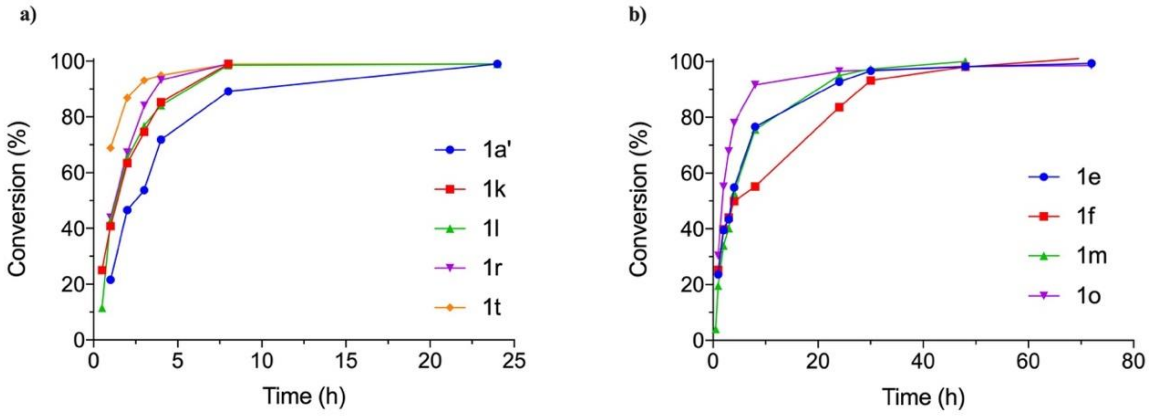

Figure 22. Time conversion profiles for the *Sc*FDC1 catalyzed decarboxylation reactions using whole cells and the optimized reaction conditions: **a)** substrates **1a'**,**k**,**l**,**r**,**t** with complete conversions in relatively short reaction time (under 24 h), **b**) substrates **1e**,**f**,**m**,**o** with complete conversions in longer reaction time (24-72 h)

The substrates **1d,h,i,j,s,v,w** reached high but incomplete conversions after 72 h (**Figure 23a.**, **Table 5B.**), and for the substrates **1g,p,q,u** moderate or low conversions were registered after 72 h (**Figure 23b.**, **Table 5B.**). Using the substrates **1n,x,y,z** no conversions were detected (**Table 5B.**).

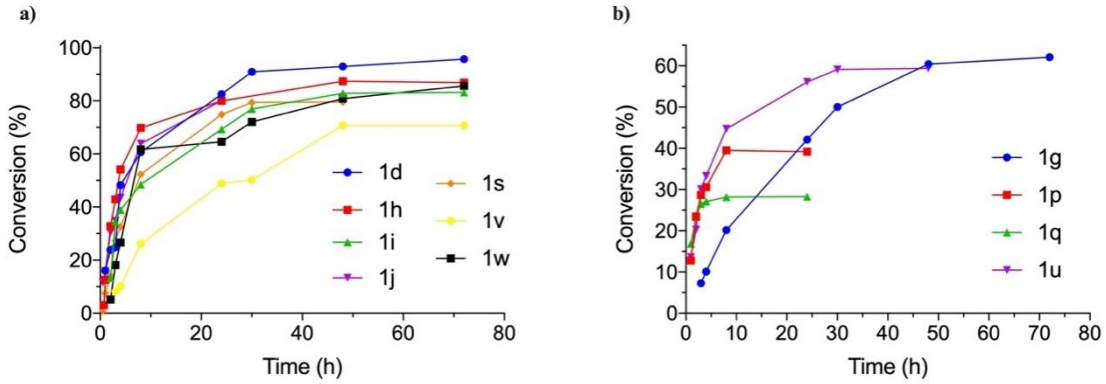

Figure 23. Time conversion profiles for the *Sc*FDC1 catalyzed decarboxylation reactions using whole cells and the optimized reaction conditions: **a**) substrates **1d,h,I,j,s,v,w** with high but incomplete conversions and; **b)** substrates **1g,p,q,u** with moderate or low conversions up to 72 h reaction time.

3.3.1.2. Computational studies

The conversion values/reaction rates are influenced by multiple substrate-related factors, such as inductive effects of substituents, presence of extended conjugation, substrate orientation related to the prFMN and within the catalytic site, the latest being influenced by both size and planarity of substrate (**Figure 24.**).

Thus we performed computational studies to determine the substrate orientation in and along the active site of the FDC1 in order to explain the differences in the conversion values of the substrates **1d-z, a'**.

Computational studies shows that in case of 5-(4-bromophenyl)furan-2-yl)acrylic acid **1x** an energetically favored, inactive substrate orientation was observed related to prFMN and the enzyme key residues (R175, E280,E285) and presumably the length of the substrate also exceeds the limits of the catalytic site for active binding position (**Figure 25a.**). The volume of the active site is also a problem in case of the substrate **1z**, where the energetically favored position of the substrate does not allow the accommodation of the substrate in the catalytic center, instead other surficial substrate binding position is observed in the proximity of the catalytic site (**Figure 26.**).

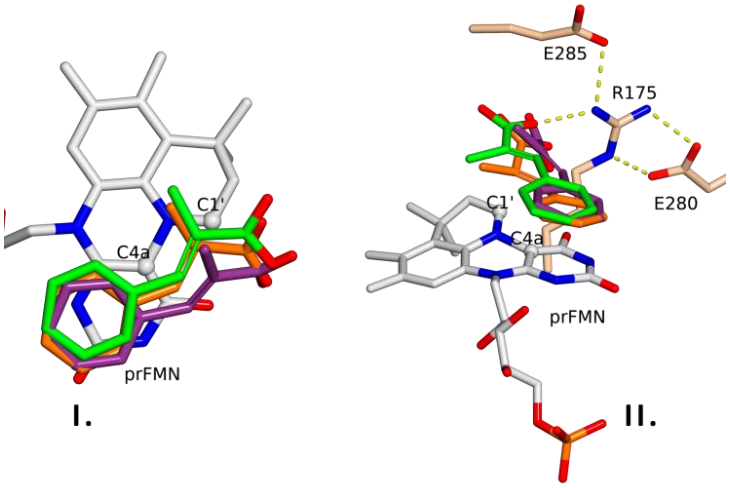

Figure 24. Comparison of ligand (α-methyl *trans*-cinnamate) conformations taken from the 4ZA7 crystal structure (violet) with the lowest energy docking pose (green), and with the reported transition state geometry[24] (orange) of 1,3-dipolar cycloaddition. **I**. – top view - the alignment of the double bond with respect to the prFMN cofactor in the docking conformation is in good agreement with the transition state geometry obtained by QM/MM study; **II**. – front view – substrate orientation related to prFMN and key residues R175, E280 and E285

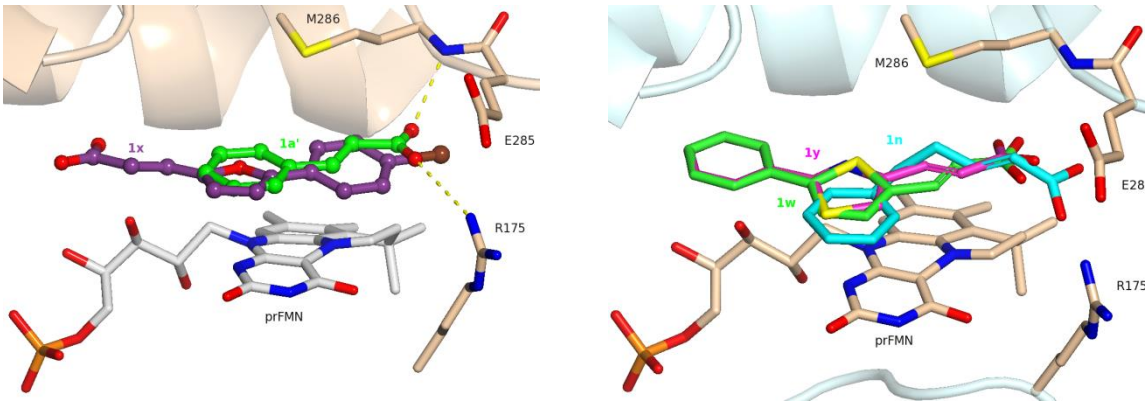

a) **b)**

Figure 25. a) The energetically favored, inactive orientation of **1x** (purple) compared to the active orientation of **1a'** (green); **b)** The inactive pose of **1y** (magenta) and **1n** (blue) within the catalytic site of FDC1, with the double bond located in an arrangement with respect to prFMN, which is unfavourable for the 1,3-cycloaddition in comparison with the productive orientation of bulky **1w** (green)

In case of (2-phenylthiazol-4-yl) acrylic acid **1y** the position of the α,β-double bond was unfavorable for the C1′ and C4a atoms of the prFMN cofactor. In the case of the substrate 5-phenylpent-2-enoic acid **1n** for which also no conversion was detected (**Table 5.**), the absence of the π-system and unfavorable arrangement of the acrylic double bond and

because of this the non-planar molecular arrangement do not let the formation of the 1,3-cycloaddition (**Figure 25b.**).

To extend the computational studies and to demonstrate that we can predict, or even more, to improve the enzyme active site for the substrates where no conversions were detected, the substrate-cofactor (prFMN) intermediates resulting after the 1,3-cycloaddition were investigated and were computed in gas phase (**Figure 27.**).

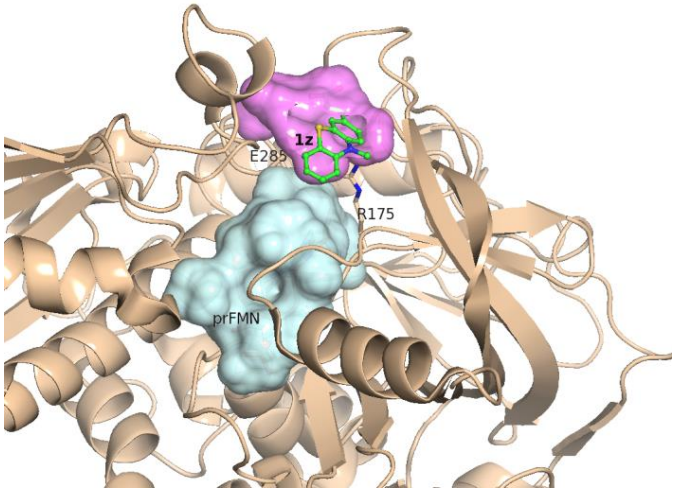

Figure 26. The energetically favored position of the substrate **1z** in the surface cavity (pink colored) located above the binding pocket (blue colored) of the FDC1 enzyme

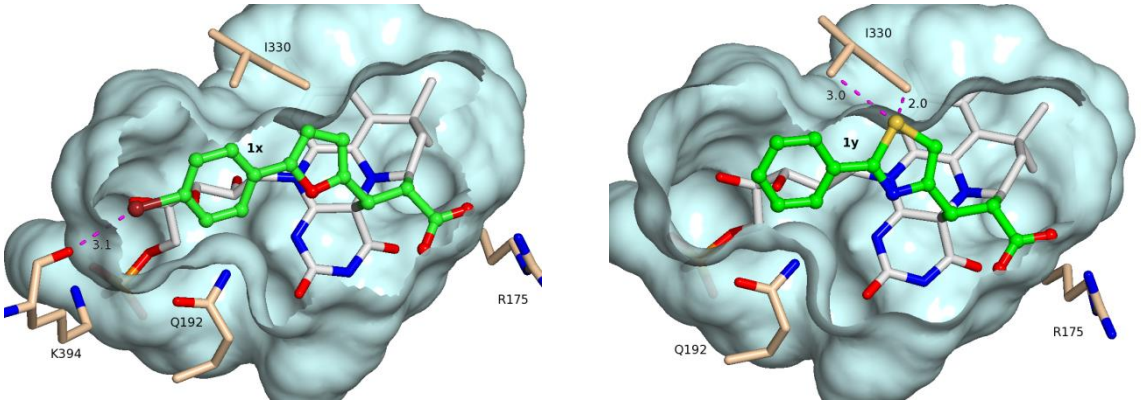

a) **b)**

Figure 27. a) Ground state conformation of substrate **1x** in the cycloadduct is hindered by the proximity of the bromine atom and the backbone carbonyl of residue K394; **b)** Steric clashes between the sulphur atom of covalent intermediate, formed by **1y** and prFMN and residue I330 are highlighted by violet dotted lines

The residues I330 and Q192 were replaced by smaller residues Ala (A), Val (V) using site-directed mutagenesis and the obtained single mutant variants were tested in the

decarboxylation reaction of bulky substrates showing steric repulsion with the gate limited by I330 and Q192 (**Table 6.**). In accordance with the computational results I330A and I330V improved the catalytic efficiency in case of the substrate **1y**, while the decreased activity of Q192N variant supports that residue Q192 is involved in binding of the prFMN cofactor.

Table 6. Conversion values with *wild-type* (wt)-*Sc*FDC1 and *Sc*FDC1 mutants for the substrates **1a',x,y,z** after 24 h

Substrate	wt-*Sc*FDC1	*Sc*FDC1 mutant		
		I330A	I330V	Q192N
	Conversion (%)			
cinnamic acid (1a')	>99	>99	>99	92
(*E*)-3-(5-(4-bromophenyl)furan-2-yl)acrylic acid (1x)	<1	<1	<1	<1
(*E*)-3-(2-phenylthiazol-4-yl)acrylic acid (1y)	<1	15	5	0
(*E*)-3-(10-methyl-10*H*-phenothiazin-2-yl)acrylic acid (1z)	<1	<1	<1	<1

3.3.1.3. Conclusions

The substrate scope of *Sc*FDC1 was explored using differently (*ortho*-, *meta*-, *para*-) substituted phenyl-, bulky heteroaryl- or biaryl-analogues of cinnamic acid, products of the biotransformation mediated by *wild-type* or engineered PALs. The results demonstrate FDC1 has a broad substrate scope with significant overlapping with the substrate scope of *Pc*PAL allowing the application of the PAL-FDC1 enzyme cascade for various substrate analogues. Molecular docking was performed to mark the correlations between the conversion values and the nature of the substrates. Based on computational studies sterical hindrance for substrate accommodation within the catalytic site of ScFDC1 has been identified, and the mutational studies provided *Sc*FDC1 variants with extended substrate scope.

3.3.2. Assembly and validation of the high-throughput fluorescent enzyme-coupled activity assay

3.3.2.1. Fluorogenic reaction set-up

Firstly we focused on the selection of reaction medium for the combined PAL-, FDC1- and 1,3-cyloaddition reactions between the tetrazole fluoroprobe and the styrene (**Figure 28.**).

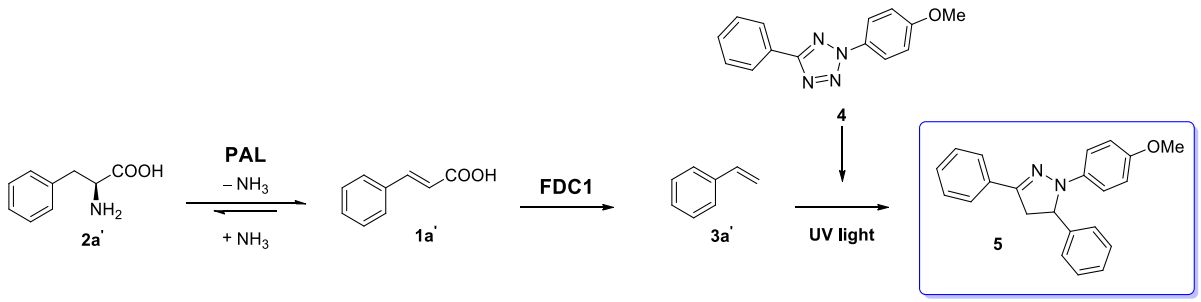

Figure 28. PAL and FDC1 coupled fluorescence assay

Accordingly, water-miscible organic solvents (acetonitrile, methanol) and/or solvents which are capable to extract the styrene from the aqueous medium (*n*-hexane) were tried in the FDC1-mediated decarboxylation reaction of cinnamic acid 1**a'**. Best fluorescence signal intensities and signal:noise *ratio* were observed when *n*-hexane was used for styrene extraction.

Next the effect of styrene **3a'** and tetrazole **4** concentrations on the fluorescence signal turn-on for the product **5** were determined using 3D excitation-emission scans (**Figure 29.**). Using the same concentration from both reaction partners (styrene **3a'** and tetrazole fluoroprobe **4**) the fluorescence signal turn-on was the highest.

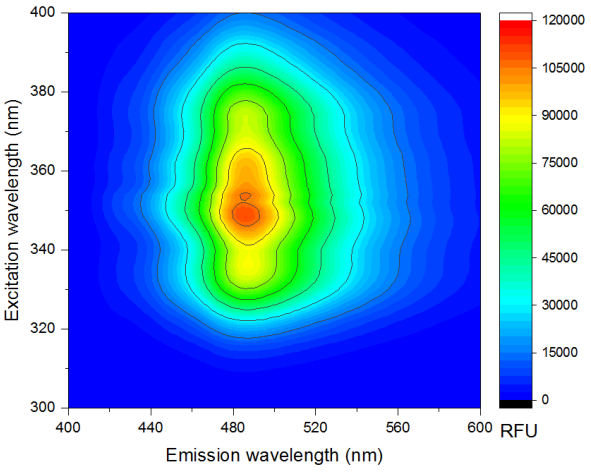

Entry	[3] (mM)	[4] (mM)	λ_{ex}^{max} (nm)	λ_{em}^{max} (nm)	FI (fold)[a]
1	1	1	355	480	402
2	0.5	0.5	350	490	432
3	0.2	0.13	362	480	38
4	0.2	0.025	362	460	13

[a]FI=fluorescence increase fold - determined from the *ratio* of signal intensities at the λ_{em}^{max} of the sample and its negative control, consisting from the UV-irradiated 4 (at the corresponding concentrations), without the presence of its reaction partner 3.

Figure 29. The effect of different styrene **3a'** and fluoroprobe **4** concentrations. The corresponding excitation and emission maxima determined by 3D excitation-emission scans

Further, it was necessary the investigation of the detection limit for the determination of PAL-activities. Therefore, calibration curves were performed (**Figure 30.**).

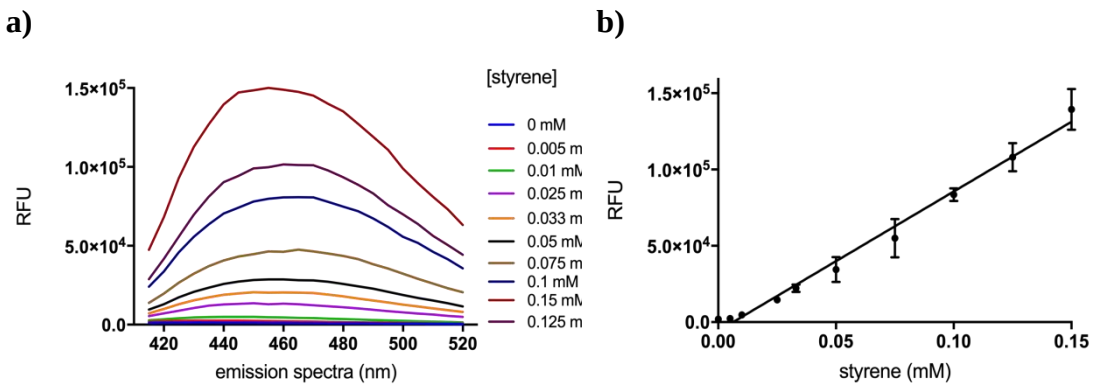

Figure 30. a) and **b)** the detection limit (defined as mean of negative controls plus three times the standard deviation of negative controls) of 25 μM styrene was obtained under a linear response up to 1 mM styrene using 0.5 mM of fluorogenic probe **4**

3.3.2.2. Coupling the PAL-, FDC1- and fluorogenic reactions

Further we tested the coupling of PAL-, FDC1- and fluorogenic reaction steps. The application of PAL-activity assay at whole cell level or cell lysates, suitable for activity analysis of clone-libraries obtained from directed evolution experiments. Mixtures of induced *E. coli* whole cells harboring the recombinant *pcpal*[25] and *scfdc1*[26] genes were tested as catalysts for the ammonia elimination of L-Phe and the subsequent decarboxylation of cinnamic acid. To rule out cell penetration issues of substrates or products, besides the whole cell-biocatalysts, the cell lysates of the induced PAL- and FDC1-whole cells were also tested.

The highest signal intensities were obtained when we used the combined reaction system (PAL- and FDC1-whole cells were added at the same time, **Figure 31.**). Moreover using cell lysates did not increase the signal intensities which suggest that no cell penetration issues are occurring.

Further, the genes encoding *Pc*PAL and *Sc*FDC1 were sub-cloned into pCDFDuet-1 vector, for their co-expression, providing a combined PAL-FDC1 whole cell-biocatalyst to exclude that the use of two separate whole cell-systems for PAL and FDC1 biocatalysts hinders the efficiency of the activity assay. The two system was compared and afforded similar results (**Figure 32a,b.**).

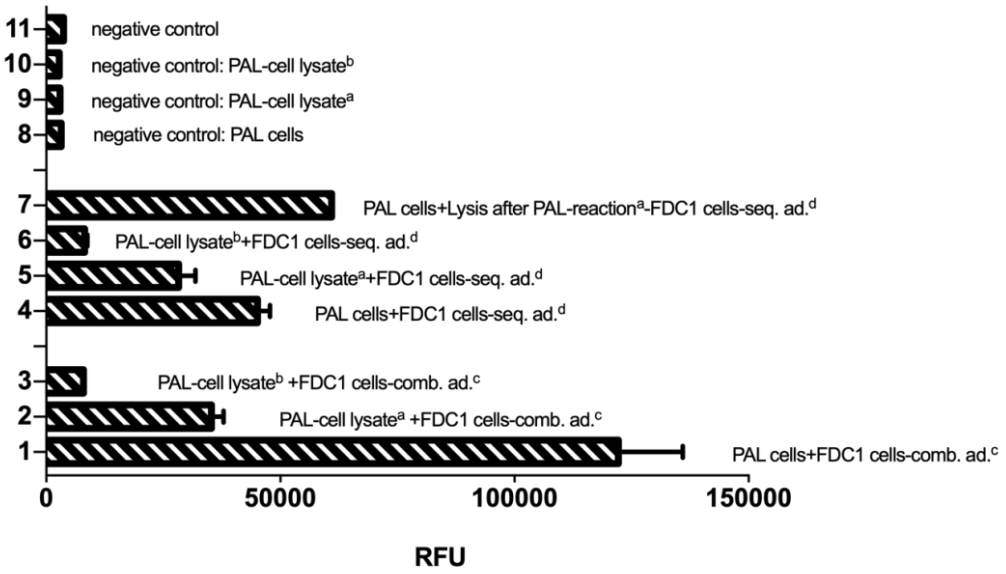

[a] lysis with polymyxin B sulphate; [b] lysis with Triton X-100; [c] combined addition of the PAL- and FDC1-biocatalysts into the reaction mixture; [d] sequential addition of FDC1- whole cells (after 12 h reaction with PAL-biocatalyst) into the assay mixture.

Figure 31. Fluorescent signal intensities for the differently coupled PAL-, FDC1- reactions

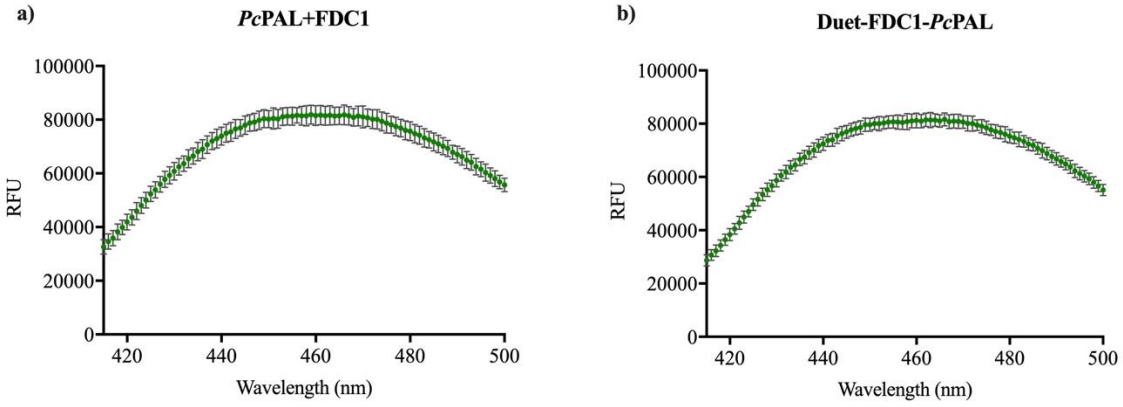

Figure 32. a) separate *Pc*PAL and FDC1 system **b)** combined *Pc*PAL-FDC1 system

3.3.2.3. Assay optimizations

The effect of pH on biotransformation

We tested the effect of pH upon the fluorescence signal intensities for the combined PAL-FDC1 reactions, because the pH optimums for the FDC1 mediated decarboxylation is at 6.5-7.0 and for the PAL catalyzed ammonia elimination reactions is at 8.0-8.5. The highest signal intensities were obtained at pH 7.5-8.0 (**Figure 33.**).

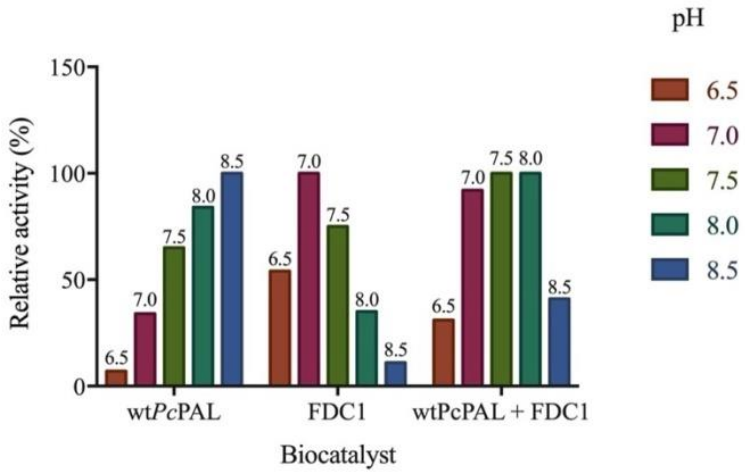

Figure 33. The determination of pH optimum of the coupled PAL-, FDC1- whole cell biotransformations in comparison with the pH optimum of the isolated *wild-type Pc*PAL-enzyme and of the FDC1-whole cell biotransformations

Effect of cells quantity on biotransformation

At optimal pH of 8.0, the effect of biocatalysts cell densities upon the fluorescence signal intensities for the combined PAL-FDC1 reactions was studied (**Figure 34.**).

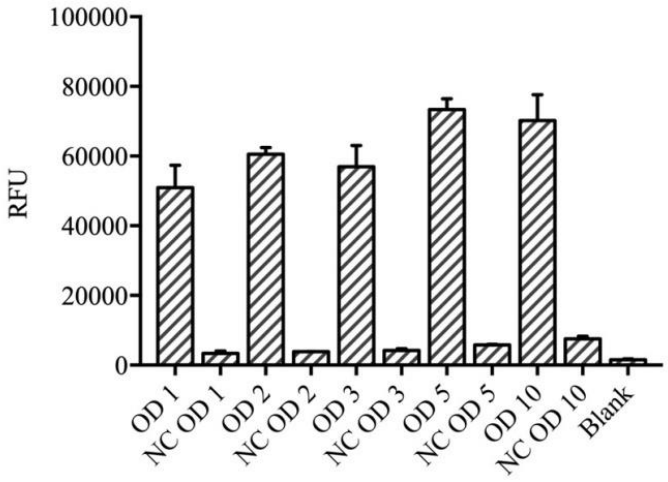

Figure 34. The effect of different cell density of FDC1 (OD_{600}~1,2,3,5,10) upon the fluorescence signal intensities using constant *Pc*PAL whole cell-concentrations of OD_{600}~1 in the combined PAL-FDC1 fluorescent activity assay. The negative controls were performed without *Pc*PAL whole cells

3.3.2.4. Method validation

To explore the applicability of the assay, we analysed the procedure using phenylalanine ammonia-lyases with different, known activities towards non-natural

substrates. Mutants of *Pc*PAL with high activity developed through rational design within this study (described at Chapter 3.2.), and the *wild-type* enzyme was tested using as model substrate the *p*-methoxy-phenylalanine. In the first study the highest PAL-activities were obtained for the mutants of *Pc*PAL I460V, I460A and F137V. In the fluorescence assay, the highest intensities were registered in the case of the same mutants (**Figure 35.**).

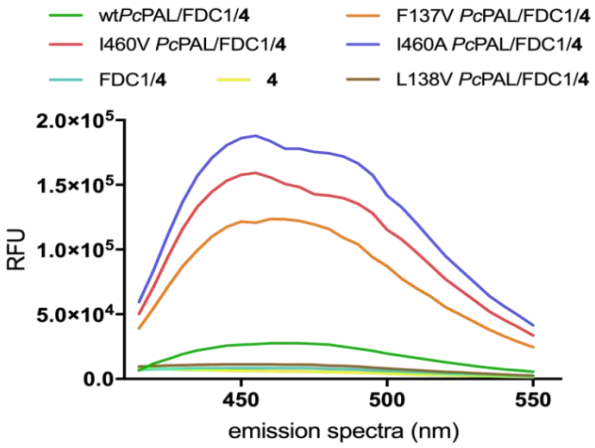

Figure 35. Fluorescence signal intensities using different *Pc*PAL mutants *p*-MeO-Phe as substrate

To further support the general applicability of the procedure, the assay was performed using whole cells harboring genes of different ammonia-lyases: PAL from *Arabidopsis thaliana* (*At*PAL) (**Figure 36a.**), tyrosine ammonia-lyase (TAL), PALs from *Rhodotorula sp.*[27], histidine ammonia-lyase (HAL) from *Pseudomonas fluorescens*[28] known as inactive towards L-tyrosine, provided signals at the level of negative controls (**Figure 36b.**).

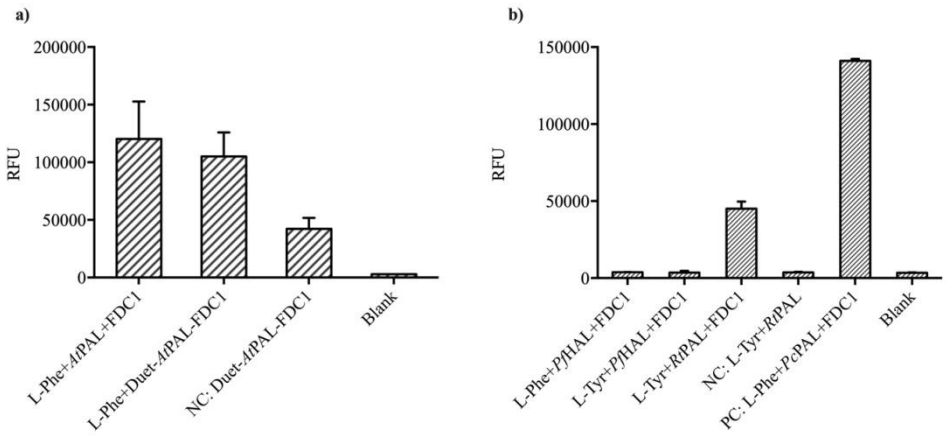

Figure 36. a) Fluorescent assay with PAL from *Arabidopsis thaliana* (*At*PAL) **b)** Fluorescent assay with PAL from *Rhodotorula toruloides* (*Rt*PAL) for TAL-activity detection

3.3.2.5. Conclusions

In this study a novel high-throughput fluorescent, enzyme-coupled assay was developed for the determination of PAL activities using the FDC1 enzyme with broad substrate range. The developed assay was successfully optimized and validated using different mutants of *Pc*PAL. The general applicability of the assay was also demonstrated using different type of ammonia-lyases such as *Pc*PAL from *Petroselinum crispum*, *At*PAL from *Arabidopsis thaliana* and *Rt*PAL from *Rhodotorula toruloides*. This high-throughput activity assay allow the testing of largely sized mutant libraries generated by directed evolution and paves the way towards PAL protein engineering.

4. General conclusions

The main aim of the study was to develop engineered PAL biocatalysts which are useful for the synthesis of several highly valuable non-natural phenylalanine analogues.

Based on existing sturctural information of PALs, firstly the mapping of the active site of *Pc*PAL through mutational analysis was developed, which revealed a correlation between the hydrophobic substrate binding site residues of the enzyme *Pc*PAL and the position (*ortho*-, *meta*-, *para*-) of the substrate's aryl ring substituent.

Since for the directed evolution of PAL enzymes high-throughput activity assays are required, in the thesis we focused also on the development of an enzyme-coupled fluorescent assay applicable for PAL-activity screens at whole cell level. The developed assay involves the enzymatic decarboxylation of *trans*-cinnamic acid (the product of the PAL reaction) by ferulic acid decarboxylase (FDC1) followed by a photochemical reaction of the produced styrene. Therefore initially for this it was needed exploring the substrate scope of ferulic acid decarboxylase for ensuring its compatibility with the substrate domain of PALs. The obtained results demonstrate that FDC1 has a broad substrate scope with significant overlap with the substrate scope of *Pc*PAL, thus supporting a successful set-up of a PAL-FDC1 enzyme cascade for various substrate analogues.

After several optimization step the high-throughput fluorescent, enzyme coupled activity assay was successfully set-up and validated on mutant *Pc*PAL libraries, as well as on PALs with different origins. Thus the developed high-throughput activity assay provide facile activity screens for the largely sized mutant libraries generated by directed evolution and paves the way towards further efficient protein engineering of phenylalanine ammonia lyases.

5. Acknowledgements

The experimental work was carried out at the laboratories of the Biocatalysis and Biotransformations Research Center, Faculty of Chemistry and Chemical Engineering of Babeș-Bolyai University.

I would first like to express my gratitude to my scientific supervisor Prof. Habil. Dr. Eng. Paizs Csaba for all his help, patience, advices, for supervising me during my research work.

Special thanks to Lect. Dr. László Csaba Bencze, who created the opportunity to learn and develop new and modern methods in our lab. Many thanks also for the financial support. I had the luck to meet a serious, hard-working, dedicated, but most importantly honest, modest, discrete and warm-heart teacher.

My sincere gratitude for the seniors of the research center: Prof. Habil. Dr. Eng. Monica Ioana Toșa, Prof. Dr. Eng. Florin Dan Irimie, Lect. Dr. Csaba Levente Nagy, Lect. Dr. Róbert Tőtős, Lect. Dr. Eng. Mădălina Elena Moisă, Assoc. Prof. Gabriel Katona, and Lect. Dr. Paula Veronica Podea, for their help during my studies and research work.

Furthermore, I would like to thank to my colleagues for their help and friendship: Assist. Prof. Eng. Souad-Diana Tork, Dr. Hajnal Vári-Bartha, Assist. Prof. Dr. Andrea Varga, Assist. Prof. Dr. Alina Filip, Assist. Prof. Dr. Melinda Emese László, Dr. Gergely Bánóczi, Cristian Andrei Gál, Eng. Adrian-Ioan Dudu, Monica Jipa, Eng. Mihai Andrei Lăcătuș, Eng. Cristina Spelmezan, Eng. Ioan Bodea, Ibolya Varga.

The work within this thesis was supported by the Swiss National Science Foundation (SNSF), through the PROMYS project, grant nr. IZ11Z0_166543 entitled “MIO-enzyme toolkit for the synthesis of unnatural amino acids” directed by Dr. László Csaba Bencze.

Last, but not least, I would like to thank to my family for their helping and loving and encouraging me.

6. List of publications

The present thesis is based on the following publications. Unpublished data is also included.

Scientific publications:

I. Moisă, M. E.; Amariei, D. A.; Nagy, E. Z. A.; Szarvas, N.; Toșa, M. I.; Paizs, C.; Bencze, L. C. Fluorescent enzyme-coupled activity assay for phenylalanine ammonia-lyases, *Scientific Reports*, **2020**, *10:18418* (impact factor: 3.998)

II. Nagy, E. Z. A.; Tork, S. D.; Lang, P. A.; Filip, A.; Irimie, F. D.; Poppe, L.; Toșa, M. I.; Schofield, C. J.; Brem, J.; Paizs, C.; Bencze, L. C. Mapping the Hydrophobic Substrate Binding Site of Phenylalanine Ammonia-Lyase from Petroselinum crispum, *ACS Catal.*, **2019**, *9*, 8825−8834 (impact factor: 12.35)

III. Nagy, E. Z. A.; Nagy, C. L.; Filip, A.; Nagy, K.; Gál, E.; Tőtős, R.; Poppe, L.; Paizs, C.;Bencze, L. C. Exploring the substrate scope of ferulic acid decarboxylase (FDC1) from *Saccharomyces cerevisiae*, *Scientific Reports*, **2019**, *9:647* (impact factor: 3.998)

Other publications resulted during my doctoral studies with complementary topics:

IV. Tork, S. D.; Nagy, E. Z. A.; Cserepes, L.; Bordea, D. M.; Nagy, B.; Toșa, M. I.; Paizs, C.; Bencze, L. C. The production of L- and D-phenylalanines using engineered phenylalanine ammonia lyases from Petroselinum crispum, *Scientific Reports*, **2019**, *9:20123* (impact factor: 3.998)

V. Filip, A.; Nagy, E. Z. A.; Tork, S. D.; Bánóczi, G.; Toșa, M. I.; Irimie, F. D.; Poppe, L.; Paizs, C.; Bencze, L. C. Tailored Mutants of Phenylalanine Ammonia-Lyase from Petroselinum crispum for the Synthesis of Bulky L- and D-Arylalanines, *ChemCatChem*, **2018**, *10*, 2627-2633 (impact factor: 4.853)

Conference presentations:

I. Nagy, E. Z. A.: *High throughput assay development for the determination of the phenylalanine ammonia-lyases activity*, National Conference of Doctoral Schools from the University Consortium, **2019**, Timișoara, Romania - oral presentation

II. Nagy, E. Z. A.: *Enantioselective production of unnatural arylalanines with mutant variants of phenylalanine ammonia from Petroselinum crispum (PcPAL) of extended substrate scope*, oral presentation at 34th Scientific Conference of Student Association (OTDK), **2019**, Budapest, Hungary

III. Nagy, E. Z. A.: *Extension of the substrate range of PcPAL phenylalanine ammonia lyase*, 20th Scientific Conference of Student Assosiations from Transylvania, **2017**, Cluj-Napoca, Romania – oral presentation – I. prize in the Organic Chemistry and Biochemistry section

IV. Nagy, E. Z. A.; Filip, A.; Bencze, L. C.; Paizs, C.; Irimie, F. D.: *Expanding the substrate range of PcPAL towards biphenyl-alanines*, poster presentation at the 16th CEEPUS Symposiumand Summer School on Bioanalysis, **2016**, Warsaw, Poland

7. References

[1] Wang, B.; Liu, Y.; Zhang, D.; Feng, Y.; Li, J. Efficient kinetic resolution of amino acids catalyzed by lipase AS '*Amano*' via cleavage of an amide bond, *Tetrahedron: Asymmetry*, **2012**, 23, 1338–1342.

[2] Ahmed, S. T.; Parmeggiani, F.; Weise, N. J.; Flitsch, S. L.; Turner, N. J. Chemoenzymatic synthesis of optically pure L- and D-biarylalanines through biocatalytic asymmetric amination and palladium-catalyzed arylation, *ACS Catal.*, **2015**, 5, 5410-5413.

[3] Gong, X.; Su, E.; Wang, P.; Wei, D. Alcaligenes faecalis penicillin G acylase-catalyzed enantioselective acylation of DL-phenylalanine and derivatives in aqueous medium, *Tetrahedron Letters*, **2011**, 52, 5398–5402.

[4] Zhang, N.; Liu, L.; Shan, G.; Cai, Q.; Lei, X.; Hong, B.; Wu, L.; Xie, Y.; Chen, R. Precursor-directed biosynthesis of new sansanmycin analogs bearing *para*-substituted-phenylalanines with high yields, *The Journal of Antibiotics*, **2016**, 1–4.

[5]Parmeggiani, F.; Weise, N. J.; Ahmed, S. T.; Turner, N. J. Synthetic and Therapeutic Applications of Ammonia-Lyases and Aminomutases, *Chem. Rev.*, **2018**, 118, 73−118.

[6] *Camm, E. L.; Neil Towers, G. H. Phenylalanine ammonia lyase, Phytochemistry, **1972,** 12 (5): 961–973.*

[7] Bartsch, S.; Bornscheuer, U. T. Mutational analysis of phenylalanine ammonia lyase to improve reactions rates for various substrates, *Protein Eng.*, **2010,** 23 (12), 929–933.

[8] Filip, A.; Nagy, E. Z. A.; Tork, S. D.; Bánóczi, G.; Toşa, M. I.; Irimie, F. D.; Poppe, L.; Paizs, C.; Bencze, L. C. Tailored mutants of phenylalanine ammonia-lyase from *Petroselinum crispum* for the synthesis of bulky L- and D-arylalanines, *ChemCatChem*, **2018**, 10, 2627-2633.

[9] Zhou, Y.; Wu, S.; Li, Z. Cascade Biocatalysis for Sustainable Asymmetric Synthesis: From Biobased L-Phenylalanine to High-Value Chiral Chemicals, *Angew. Chem. Int. Ed.*, **2016**, 55, 1-5.

[10] Wang, Y.; Song, W.; Hu, W. J.; Lin, Q. Fast Alkene Functionalization In Vivo by Photoclick Chemsitry: HOMO Lifting of Nitrile Imine Dipoles, *Angew. Chem. Int. Ed.*, **2009**, 48, 5330-5333.

[11] Parmeggiani, F.; Lovelock, S. L.; Weise, N. J.; Ahmed, S. T.; Turner, N. J. Synthesis of D- and L-phenylalanine derivatives by phenylalanine ammonia lyases: a multienzymatic cascade process, *Angew. Chem. Int. Ed.*, **2015**, 54, 4608-4611.

[12] Claypool, J. T.; Raman, D. R.; Jarboe, L. R.; Nielsen, D. R. Technoeconomic evaluation of bio-based styrene production by engineered *Escherichia coli*, *J. Ind. Microbiol. Biotechnol.*,**2014**.

[13] McKenna, R.; Nielsen, D. R. Styrene biosynthesis from glucose by engineered, E. coli. *Metab. Eng.*, **2011**, 13, 544–554.

[14] Peng, A.; Qing, L. Sterically shielded tetrazoles for fluorogenic photoclick reaction: Tuning cycloaddition rate and product fluorescence, *Org. Biomol. Chem.*, **2013**, 00, 1-3.

[15] Zhi, L. Y.; Sarada, S. R.; Farid, J. G.; Yin, N. T. Rapid and sensitive detection of acrylic acid using a novel fluorescence assay, *RSC Adv.*, **2014**, 4, 60216-60220.

[16] Wang, Y.; Song, W.; Hu, W. J.; Lin, Q. Fast Alkene Functionalization In Vivo by Photoclick Chemsitry: HOMO Lifting of Nitrile Imine Dipoles, *Angew. Chem. Int. Ed.*, **2009**, 48, 5330-5333.

[17] Ferguson, K. L.; Arunrattanamook, N.; Marsh, E. N. G. Mechanism of the novel prenylated flavin-containing enzyme ferulic acid decarboxylase probed by isotope effects and linear free-energy relationships, *Biochemistry*, **2016**, 55, 2857–2863.

[18] Wang, Y. S.; Fang, X.; Chen, H. Y.; Wu, B.; Wang, Z. U.; Hilty, C.; Liu, W. R. Genetic Incorporation of Twelve meta-Substituted Phenylalanine Derivatives Using a Single Prrolysyl-tRNA Synthetase Mutant, *ACS Chem. Biol*, **2013**, 8, 405−415.

[19] Rowles, I.; Groenendaal, B.; Binay, B.; Malone, K. J.; Willies, S. C.; Turner, N. J. Engineering of phenylalanine ammonia lyase from *Rhodotorula graminis* for the enhanced synthesis of unnatural L-amino acids, *Tetrahedron*, **2016**, 72, 7343-7347.

[20] Wakiec, R.; Gabriel, I.; Prasad, R.; Becker, J. M.; Payne, J. W.; Milewski, S.Enhanced Susceptibility to Antifungal Oligopeptides in Yeast Strains Overexpressing ABC Multidrug Efflux Pumps, *Antimicrob. Agents Chemother.*,2008, 52, 4057–4063.

[21] Schroeder, A. C.; Kumaran S.; Hicks, L. M.; Cahoon, R. E.; Halls, C.; Yu, O.; Jez, J. M. Contributions of conserved serine and tyrosine residues to catalysis, ligand binding, and cofactor processing in the active site of tyrosine ammonia lyase, *Phytochemistry*, **2008**, 69, 1496-1506.

[22] Rowles, I.; Groenendaal, B.; Binay, B.; Malone, K. J.; Willies, S. C.; Turner, N. J. Engineering of phenylalanine ammonia lyase from *Rhodotorula graminis* for the enhanced synthesis of unnatural L-amino acids, *Tetrahedron*, **2016**, 72, 7343-7347.

[23] Yan, C.; Parmeggiani, F.; Jones, E. A.; Claude, E.; Hussain, S. A.; Turner, N. J.; Flitsch, S. L.; Barran, P. E. Real-time screening of biocatalysts in live bacterial colonies, *J. Am. Chem. Soc.*, **2017**, 139, 1408-1411.

[24] Lan, C.-L.; Chen, S.-L. The decarboxylation of *α,β*-unsaturated acid catalyzed by prenylated FMN-dependent ferulic acid Decarboxylase and the enzyme inhibition,*J. Org. Chem.*, **2016**, 81, 9289–9295.

[25] Paizs, C.; Toşa, M. I.; Bencze, L. C.; Brem, J.; Irimie, F. D.; Rétey, J. 2-amino-3-(5-phenylfuran-2-yl)propionic acids and 5-phenylfuran-2-ylacrylic acids are novel substrates of phenylalanine ammonia-lyase, *Heterocycles*, **2010**, 82, 1217-1228.

[26] Ahmed, S. T.; Parmeggiani, F.; Weise, N. J.; Flitsch, S. L.; Turner, N. J. Engineered ammonia lyases for the production of challenging electron-rich L-phenylalanines, *ACS Catal.*, **2018**, 8, 3129-3132.

[27] Dreßen, A.; Hilberath, T.; Mackfeld, U.; Billmeier, A.; Rudat, J.; Pohl, M. Phenylalanine ammonia lyase from *Arabidopsis thaliana* (*At*PAL2): A potent MIO-enzyme for the synthesis of non-canonical aromatic alpha-amino acids: Part I: Comparative characterization to the enzymes from *Petroselinum crispum* (*Pc*PAL1) and *Rhodosporidium toruloides* (*Rt*PAL), *J. Biotechnol.*, **2017**, 258, 148-157.

[28] Csuka, P.; Juhász, V.; Kohári, S.; Filip, A.; Varga, A.; Sátorhelyi, P.; Bencze, L. C.; Barton, H.; Paizs, C.; Poppe, L. *Pseudomonas fluorescens* Strain R124 Encodes Three Different MIO Enzymes, *ChemBioChem*, **2018**, 19, 411-418.